



## Identification of a potent and selective phosphatidylinositol 3-kinase $\delta$ inhibitor for the treatment of non-Hodgkin's lymphoma

Wei-Qiong Zuo<sup>a,b,1</sup>, Rong Hu<sup>a,1</sup>, Wan-Li Wang<sup>a</sup>, Yong-Xia Zhu<sup>b</sup>, Ying Xu<sup>b</sup>, Luo-Ting Yu<sup>b</sup>, Zhi-Hao Liu<sup>b,\*</sup>, Ning-Yu Wang<sup>a,\*</sup>

<sup>a</sup> School of Life Science and Engineering, Southwest Jiaotong University, Chengdu, China

<sup>b</sup> Lab of Medicinal Chemistry, Cancer Center, West China Hospital, Sichuan University and Collaborative Innovation Center, Chengdu, China

### ARTICLE INFO

#### Keywords:

Non Hodgkin's lymphoma  
PI3K $\delta$  inhibitor  
Antiproliferative  
Apoptosis  
Piperazinone  
Purine

### ABSTRACT

PI3K $\delta$  has proved to be an effective target for anti-lymphoma drugs. However, the application of current approved PI3K $\delta$  inhibitors has been greatly limited due to their specific immune-mediated toxicity and increased risk of infection, it is necessary to develop more PI3K $\delta$  inhibitors with new scaffold. In this study, SAR study with respect to piperazinone-containing purine derivatives led to the discovery of a potent and selective PI3K $\delta$  inhibitor, 4-(cyclobutanecarbonyl)-1-((2-(2-ethyl-1*H*-benzo[*d*]imidazol-1-yl)-9-methyl-6-morpholino-9*H*-purin-8-yl)methyl)piperazin-2-one (**WNY1613**). **WNY1613** exhibits good antiproliferative activity against a panel of non-Hodgkin's lymphoma (NHL) cell lines by inducing cancer cell apoptosis and inhibiting the phosphorylation of PI3K and MAPK downstream components. In addition, it can also prevent the tumor growth in both SU-DHL-6 and JEKO-1 xenograft models without observable toxicity. **WNY1613** thus could be developed as a promising candidate for the treatment of NHL after subsequent extensive pharmacodynamics and pharmacokinetics investigation.

### 1. Introduction

Members of the phosphoinositide 3-kinase (PI3K) family catalyze the phosphorylation of phosphatidylinositol 4,5-diphosphate (PIP<sub>2</sub>) to produce phosphatidylinositol 3,4,5-triphosphate (PIP<sub>3</sub>), which acts as a second messenger to transduce extracellular signals into cells by interacting with a variety of pH domain-containing proteins [1–2]. PI3K $\delta$  is an isoform of PI3K family which mainly expresses in leukocytes and regulates many crucial physiological processes of leukocytes as well as malignant lymphoma cells [3–5]. It is therefore considered as a potential therapeutic target for several kinds of lymphomas, including chronic lymphocytic leukemia (CLL) and non Hodgkin's lymphomas (NHLs) [6].

In the last decade, a number of PI3K $\delta$  inhibitors have been developed and entered into clinical trials [7–9]. Several promising candidates, including the selective PI3K $\delta$  inhibitor Idelalisib as well as the partial isoforms selective PI3K $\delta$  inhibitors Duvelisib and Copanlisib (Fig. 1) [10–12], have been approved for the treatment of follicular B-cell non-Hodgkin lymphoma (FL), small lymphocytic lymphoma (SLL) and chronic lymphocytic leukemia (CLL). Although these PI3K $\delta$  inhibitors

exhibited impressive therapeutic efficiency, specific immune-mediated toxicity and increased risk of infection prevented their widespread application [8,13]. As most PI3K $\delta$  inhibitors that are approved or in advanced clinical trials are similar in structure [9], it is difficult to determine whether their adverse events observed in clinical are structural related or target related. More structurally diverse PI3K $\delta$  inhibitors thus need to be developed.

We recently discovered that piperazinone-containing thieno[3,2-*d*]pyrimidine was a promising scaffold for PI3K $\delta$  inhibitors, and the piperazinone fragment in this series played important roles in improving the PI3K $\delta$  potency and the  $\delta$  isoform selectivity [14]. The preliminary SAR study has led to the discovery of several potent and selective PI3K $\delta$  inhibitors with single-digit nanomolar IC<sub>50</sub> values and selectivity index of over 100 folds against other three PI3K isoforms. Because previous studies had demonstrated that purine ring would be a better scaffold for this kind of PI3K $\delta$  inhibitors with respect to their isoform selectivity as well as pharmacokinetic properties (**GNE-293**, for example) [15–16], we speculated that the replacement of thieno[3,2-*d*]pyrimidine core with purine ring would result in a new series of PI3K $\delta$  inhibitors with

\* Corresponding authors.

E-mail addresses: [liuzhihao@scu.edu.cn](mailto:liuzhihao@scu.edu.cn) (Z.-H. Liu), [wangny-swjtu@swjtu.edu.cn](mailto:wangny-swjtu@swjtu.edu.cn) (N.-Y. Wang).

<sup>1</sup> These authors contributed equally to this work.

improved potency and drug-like properties (Fig. 2).

In this study, a series of 4-((9-methyl-9H-purin-8-yl)methyl)piperazin-2-ones and 1-((9-methyl-9H-purin-8-yl)methyl)piperazin-2-ones were designed and synthesized as PI3K $\delta$  inhibitors (Fig. 2). SAR study led to the discovery of the most promising candidate **WNY1613**, which exhibited good target affinity and selectivity. Here we report the discovery, the biological activity evaluation as well as the mechanism of action (MOA) studies with respect to this PI3K $\delta$  inhibitor in several NHLs models.

## 2. Results and discussion

### 2.1. Chemistry

The title compounds mentioned in this study were prepared according to a similar synthetic route for the preparation of piperazinone-containing thieno[3,2-*d*]pyrimidine PI3K $\delta$  inhibitors [14]. As shown in Scheme 1, nucleophilic substitution and methylation of compound **1** provided 4-(2-chloro-9-methyl-9H-purin-6-yl)morpholine (**2**), which underwent formylation with dimethylformamide and subsequent reduction with sodium borohydride to afford intermediate **3**. The alcohol **3** then coupled with 2-ethylbenzo[*d*]imidazole to provide **4**, which was further chloridized with thionyl chloride to yield intermediates **5**. The title compounds **7a-7d** was prepared by nucleophilic substitution of **5** with different 1-substituted piperazin-2-ones [14,17]. And the critical building block **6** was prepared by nucleophilic substitution of **5** with *tert*-butyl 3-oxopiperazine-1-carboxylate and subsequent deprotection step of boc group with trifluoroacetic acid. Then, it was reacted with 2,2,2-trifluoroethyl methanesulfonate to produce **8a** or underwent reduction amination with different ketones to produce **8b-8i**. Deprotecting ethylene glycol of **8i** with concentrated hydrochloric acid provided ketone **8j**, which was further reduced by sodium borohydride to provide **8k**. Finally, the acyl derivatives **8l-8q** were prepared by acylation reaction of **6** with different acyl chlorides, and the sulfonyl substituted derivatives **8r-8t** were prepared by sulfonylation reaction of **6** with different sulfonyl chlorides.

### 2.2. The discovery of **WNY1613**

A series of 4-((9-methyl-9H-purin-8-yl)methyl)piperazin-2-ones and 1-((9-methyl-9H-purin-8-yl)methyl)piperazin-2-ones were synthesized in this study. As shown in Table 1, both 4-((9-methyl-9H-purin-8-yl)methyl)piperazin-2-one series (**7a-7d**) and 1-((9-methyl-9H-purin-8-yl)methyl)piperazin-2-one series (**8a-8t**) exhibited excellent PI3K $\delta$  inhibitory activity with moderate to good  $\delta$  isoform selectivity. An acyl substituted at the 4-position of piperazinone (**8l-8q**) in the 1-((9-methyl-9H-purin-8-yl)methyl)piperazin-2-one series seem to be conducive to the improvement of both potency and selectivity, while the alkyls (**8a-8k**) and sulfonyls (**8r-8t**) substituted series exhibited less selectivity for PI3K $\alpha$ .

To identify a lead compound from the abovementioned compounds for subsequent biological evaluation, several potent compounds were

selected to further evaluate their isoforms selectivity for PI3K $\beta$  and PI3K $\gamma$  as well as their antiproliferative activity against mantle cell lymphoma (MCL) cell line JEKO-1 by MTT assay (Table 2). Most compounds exhibited good  $\delta/\beta$  and  $\delta/\gamma$  selectivity and good antiproliferative activity against JEKO-1 with submicromolar IC<sub>50</sub> values. Of these compounds, **8p** (**WNY1613**) was selected for further biological evaluation for its excellent potency and selectivity for PI3K $\delta$  as well as good antiproliferative activity against JEKO-1.

### 2.3. Biochemical characterization of **WNY1613**

To further evaluate the target selectivity of **WNY1613**, we next evaluated the inhibitory activity of **WNY1613** on a panel of 300 kinases. **WNY1613** only exhibited potency (>50%) against the four PI3K isoforms at a concentration of 500 nM, while no inhibitory activity was observed for other kinases (Fig. 3A, B). Cellular thermal shift assay (CETSA) could evaluate the potential direct interaction between protein and its ligand [20]. We next evaluated the effect of **WNY1613** on the thermal stability of PI3K $\delta$ . The result showed that **WNY1613** could significantly improve the thermal stability of PI3K $\delta$  at a concentration of 10  $\mu$ M, implying the direct interaction between **WNY1613** and PI3K $\delta$  (Fig. 3C). Overall, these results indicated that **WNY1613** was a potent and highly selective PI3K $\delta$  inhibitor.

### 2.4. Molecular docking

The binding modes of **WNY1613** with PI3K $\delta$  (PDB ID: 2WXP) [21] and PI3K $\gamma$  (PDB ID: 3DBS) [22] were then investigated by molecular docking. As shown in Fig. 4, the morpholine and benzimidazole motifs of **WNY1613** adopt highly similar conformations in both PI3K $\delta$  and PI3K $\gamma$ , and the morpholine O atom of **WNY1613** forms a crucial hydrogen bond with both Val828 in PI3K $\delta$  and Val882 in PI3K $\gamma$ , respectively. However, an additional hydrogen bond could be exclusively formed between the piperazinone O atom of **WNY1613** and Asn836 of PI3K $\delta$ . Moreover, the bulky cyclobutanecarbonyl motif of **WNY1613** could stack on the "tryptophan shelf" formed by Thr750 and Trp760 in PI3K $\delta$  while it could not be well accommodated in PI3K $\gamma$  in which the small threonine (Thr750) is replaced by a larger, charged lysine (Lys802) [16]. These results thus explained the excellent PI3K $\delta$  potency of **WNY1613** and its well PI3K $\delta$  selectivity over other PI3K isoforms.

### 2.5. Antiproliferative activity of **WNY1613**

We next selected 10 different types of NHL cell lines, including seven diffuse large B-cell lymphoma (DLBCL) cell lines (SU-DHL-6, SU-DHL-4, OCI-LY-3, OCI-LY-10, U2932, WSU-DLCL-2, DB), two mantle cell lymphoma (MCL) cell lines (JEKO-1, Granta-519) and one Burkitt's lymphoma (NAMALVA) cell line, to investigate their sensitivity to **WNY1613** by MTS assay. As shown in Table 3, several NHL cell lines, including SU-DHL-6, SU-DHL-4, JEKO-1, OCI-LY-3, Granta-519 and NAMALVA, were sensitive to both Idelalisib and **WNY1613** with micromolar to sub-micromolar IC<sub>50</sub> values, and the antiproliferative

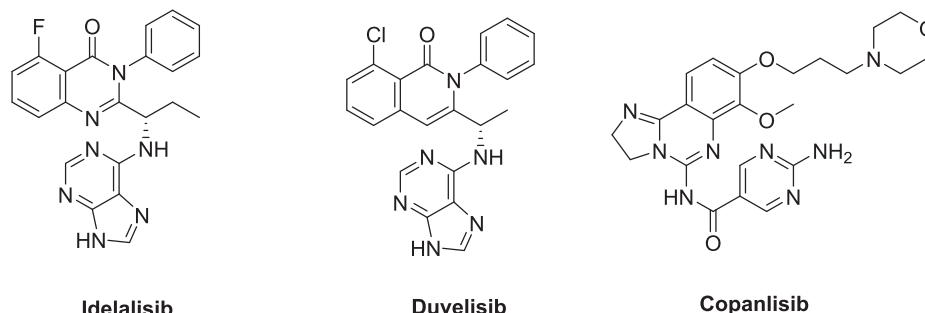


Fig. 1. Structure of three approved PI3K $\delta$  inhibitors.

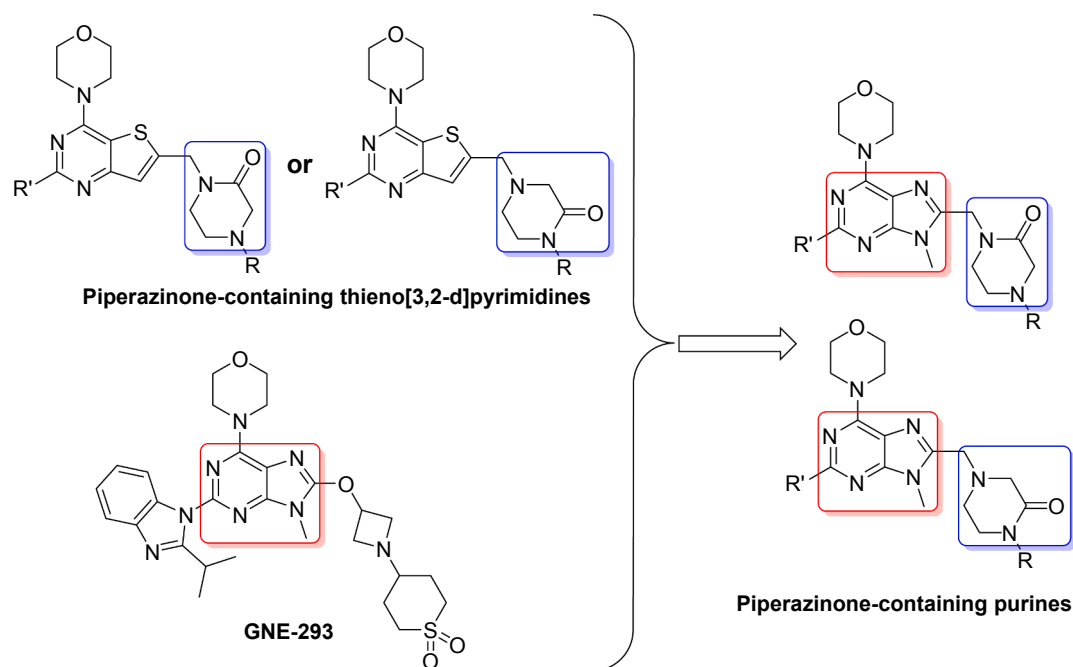
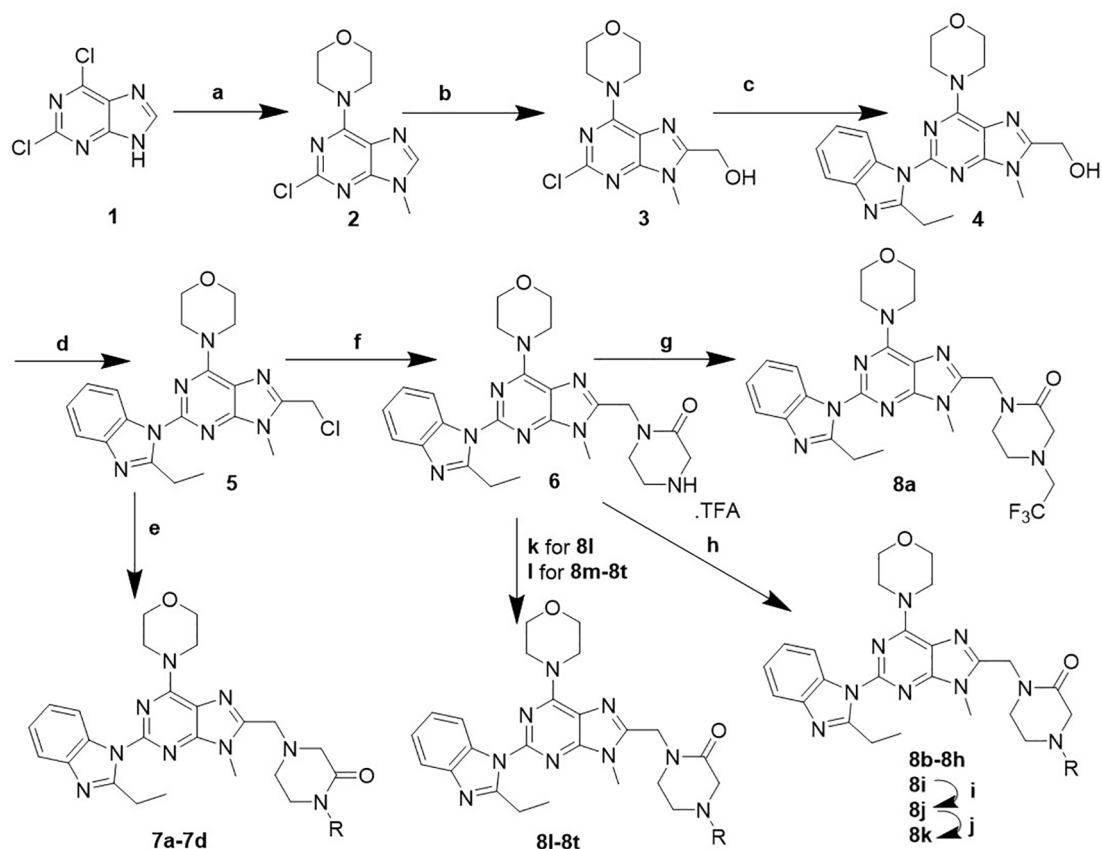
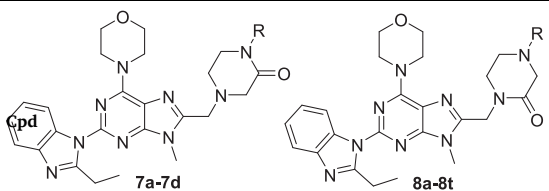


Fig. 2. Design of piperazinone-containing purines as PI3K $\delta$  inhibitors, GNE-293 is a potent and selective PI3K $\delta$  inhibitor with purine core [16].



**Scheme 1.** Synthesis of purine derivatives 7a-7d and 8a-8 t. Reagents and conditions: (a). morpholine, MeOH, rt; ② methyl iodide, MeCN, Cs<sub>2</sub>CO<sub>3</sub>, rt. (b). *n*-BuLi, DMF, THF, -78°C; ② NaBH<sub>4</sub>, MeOH. (c). 2-ethyl-1*H*-benzo[*d*]imidazole, Pd<sub>2</sub>(dba)<sub>3</sub>, XPhos, Cs<sub>2</sub>CO<sub>3</sub>, 1,4-dioxane, 110°C. (d). thionyl chloride, DCM. (e). 1-substituted piperazin-2-ones, DIPEA, *i*-PrOH, reflux. (f). *N*-*tert*-butoxycarbonyl-3-oxopiperazine, *t*-BuOK, THF, 0°C; ② TFA, DCM, rt. (g). 2,2,2-trifluoroethyl methanesulfonate, K<sub>2</sub>CO<sub>3</sub>, MeCN, reflux. (h). aldehydes or ketones, DCM, sodium triacetoxyborohydride. (i). DCM, THF, concentrated HCl(aq). (j). NaBH<sub>4</sub>, MeOH, 0°C- r.t. (k). *l*-lactic acid, HOBT, EDCI, TEA, DCM. (l). acyl chlorides or sulfonyl chlorides, TEA, DCM.

**Table 1**  
SAR study of piperazinone-containing purine PI3K $\delta$  inhibitors.

		PI3K $\delta$ <sup>a</sup> IC <sub>50</sub> (nM)	Selectivity fold over PI3K $\alpha$ <sup>b</sup>	Cpd	R	PI3K $\delta$ IC <sub>50</sub> (nM)	Selectivity fold over PI3K $\alpha$
7a		5.1 ± 1.7	77	8j		6.6 ± 3.1	63
7b		3.4 ± 1.5	96	8k		3.3 ± 0.6	68
7c		4.4 ± 2.1	81	8l		2.7 ± 1.7	83
7d		8.6 ± 2.4	43	8m		1.6 ± 0.8	148
8a		5.1 ± 0.7	68	8n		2.1 ± 1.1	134
8b		4.8 ± 1.3	66	8o		1.8 ± 0.9	126
8c		11 ± 3.8	44	8p		1.2 ± 0.7	219
8d		4.5 ± 2.2	65	8q		4.6 ± 1.9	86
8e		4.2 ± 0.6	35	8r		2.7 ± 1.3	52
8f		2.7 ± 1.1	91	8s		6.9 ± 0.7	37
8g		2.7 ± 1.4	86	8t		3.2 ± 1.4	50
8h		2.0 ± 0.8	47	PI-103 <sup>c</sup>		6.2 ± 2.7	1.6
8i		2.3 ± 0.4	58	Idelalisib <sup>d</sup>		4.7 ± 2.6	>106

<sup>a</sup> IC<sub>50</sub> values for PI3K $\delta$  are the mean of three independent measurements and that for PI3K $\alpha$  are the mean of at least two independent measurements.

<sup>b</sup> The selectivity fold over PI3K $\alpha$  was calculated as the ratio of the IC<sub>50</sub> values of a compound to PI3K $\alpha$  and PI3K $\delta$ .

<sup>c</sup> PI-103 is a pan-PI3K inhibitor with reported IC<sub>50</sub>s of 2 nM and 3 nM against PI3K $\alpha$  and PI3K $\delta$ , respectively [18].

<sup>d</sup> The reported IC<sub>50</sub>s for Idelalisib against PI3K $\alpha$ ,  $\beta$ ,  $\delta$  and  $\gamma$  were 820 nM, 565 nM, 2.5 nM and 89 nM, respectively [19].

activity of **WNY1613** was better than Idelalisib to different extent across all these sensitive cell lines, which is consistent with its better PI3K $\delta$  potency than Idelalisib.

## 2.6. Apoptosis induction activity of **WNY1613**

Apoptosis induction is a common mechanism to mediate the anti-proliferative activity of kinase inhibitors, including PI3K inhibitors [23–24]. We next assessed the apoptosis induction effect of **WNY1613** on four NHL cell lines, including SU-DHL-6, SU-DHL-4, JEKO-1, and NAMALVA. As shown in Fig. 5, **WNY1613** could induce cancer cell apoptosis (Annexin V-positive) across all four NHL cell lines in a concentration-dependent manner. And the apoptosis induction effect of **WNY1613** was also more obvious than that for Idelalisib. We next evaluated the protein levels of the apoptosis cascade, and the results showed that **WNY1613** could reduce the expression of anti-apoptotic protein BCL-2 and increase the expression of pro-apoptotic protein BAX as well as cleaved caspase-3 in a concentration-dependent manner (Fig. 5C). And the effects of **WNY1613** on the protein level of the apoptosis cascade was also more significant than that for Idelalisib across all four NHL cell lines, which was consistent with its better

apoptosis induction effects. Moreover, the apoptosis induction effects of **WNY1613** and Idelalisib as well as their influence on the protein level of the apoptosis cascade in NAMALVA cells were significantly weaker than that in other three cell lines, which could explain the weaker anti-proliferative activity of both compounds on NAMALVA cells as compared with other three cell lines.

## 2.7. PI3K pathway inhibition by **WNY1613**

The PI3K downstream components, AKT, S6, 4EBP1, as well as the MAPK downstream component ERK have been reported to be phosphorylated by PI3K activation [25], which could promote the proliferation of lymphoma cells. We next examined the effects of Idelalisib and **WNY1613** on the expression of these proteins by western blotting. Both Idelalisib and **WNY1613** could inhibit the phosphorylation of AKT, S6, 4EBP1 and ERK in a dose- and time-dependent manners without affecting their total protein levels (Fig. 6). And the inhibitory effects of **WNY1613** on the phosphorylation of these proteins were more significant than Idelalisib in all four cell lines. In addition, consistent with the results in antiproliferative assay and apoptosis induction test, the phosphorylation of PI3K pathway-related proteins in NAMALVA cells

**Table 2**

The PI3K isoforms selectivity and antiproliferative activity of piperazinone-containing purine PI3K $\delta$  inhibitors<sup>a</sup>.

Cmpds	PI3K $\delta$ (IC <sub>50</sub> : nM)	PI3K $\alpha$ selectivity	PI3K $\beta$ selectivity	PI3K $\gamma$ selectivity	JEKO- 1 (IC <sub>50</sub> : $\mu$ M)
7b	3.4 $\pm$ 1.5	96	>147	>147	0.20 $\pm$ 0.08
8f	2.7 $\pm$ 1.1	91	133	96	0.37 $\pm$ 0.06
8l	2.7 $\pm$ 1.7	83	10	96	0.28 $\pm$ 0.13
8m	1.6 $\pm$ 0.8	148	27	169	0.28 $\pm$ 0.10
8n	2.1 $\pm$ 1.1	134	238	207	0.23 $\pm$ 0.14
8o	1.8 $\pm$ 0.9	126	77	60	0.18 $\pm$ 0.05
8p (WNY1613)	1.2 $\pm$ 0.7	219	120	250	0.14 $\pm$ 0.07
Idelalisib	4.7 $\pm$ 2.6	>106	>106	52	0.93 $\pm$ 0.54

<sup>a</sup> IC<sub>50</sub> values for PI3K $\delta$  isoforms and antiproliferative activity against JEKO-1 are the mean of at least three independent measurements.

was also minimally affected by both compounds across all four cell lines, implying that the antiproliferative effect of WNY1613 is mainly mediated by its inhibition on PI3K pathway.

## 2.8. In vivo efficacy of WNY1613

To evaluate the in vivo anti-tumor activity of WNY1613, SU-DHL-6 and JEKO-1 cells were subcutaneously engrafted into NOD-SCID mice to establish xenograft models. As shown in Fig. 7, tumor-bearing mice were oral administration of WNY1613 with dosages of 25 and 50 mg/kg, Idelalisib with dosage of 25 mg/kg, or the vehicle for 18 days. The results showed that both Idelalisib and WNY1613 demonstrated solid antitumor activity in both xenograft models at a dose of 25 mg/kg, with tumor growth inhibition (TGI) rates of 47.69% and 51.38% for SU-DHL-6 model and 45.92% and 55.52% for JEKO-1 model, respectively.

Increasing the dosage of WNY1613 to 50 mg/kg only slightly increased the TGI in the JEKO-1 model, which might be attributed to the poor pharmacokinetic properties of WNY1613 in its current dosage form. Moreover, no apparent body weight loss or abnormal behavior was observed during the treatment period (Fig. 7C), implying the good safety profile of WNY1613.

To investigate the underlying mechanisms of the in vivo antitumor effects of WNY1613, immunohistochemical analysis was performed for tumor tissues resected from both tumor models after drug withdrawal. As shown in Fig. 7D and E, a significant reduction of p-AKT, p-P70S6K, p-4EBP1 and p-ERK was observed in the Idelalisib and WNY1613 groups than the vehicle group, indicating that WNY1613 could inhibit PI3K pathway in vivo. Overall, the in vivo pharmacodynamics study further confirmed the solid anticancer activity of WNY1613 via its inhibition on PI3K.

## 2.9. Conclusion

A potent PI3K $\delta$  inhibitor WNY1613 based on piperazinone-containing purine scaffold was discovered from our SAR study. This compound exhibited excellent target affinity and isoforms selectivity with IC<sub>50</sub> of 1.2 nM against PI3K $\delta$  and selectivity index of over 100 folds for other PI3K isoforms. The direct interaction between WNY1613 and PI3K $\delta$  was further validated by cellular thermal shift assay. WNY1613 could inhibit the proliferation of several NHL cell lines with micromolar to sub-micromolar IC<sub>50</sub> values. The MOA study demonstrated that it could induce apoptosis of lymphoma cells by reducing the expression of anti-apoptotic proteins and increasing the expression of pro-apoptotic proteins. Moreover, as a PI3K $\delta$  inhibitor, WNY1613 can inhibit the phosphorylation of PI3K downstream components AKT, S6, 4EBP1 and MAPK downstream component ERK in a concentration- and time-dependent manners. Finally, WNY1613 demonstrated solid antitumor activity in both SU-DHL-6 and JEKO-1 xenograft models without observable toxicity. Overall, our study provided a potent PI3K $\delta$  inhibitor WNY1613 as a promising candidate for lymphoma. The optimization of its dosage form would further improve its effectiveness in vivo and further pharmacodynamic studies in more lymphoma models would promote its development as a preclinical candidate.

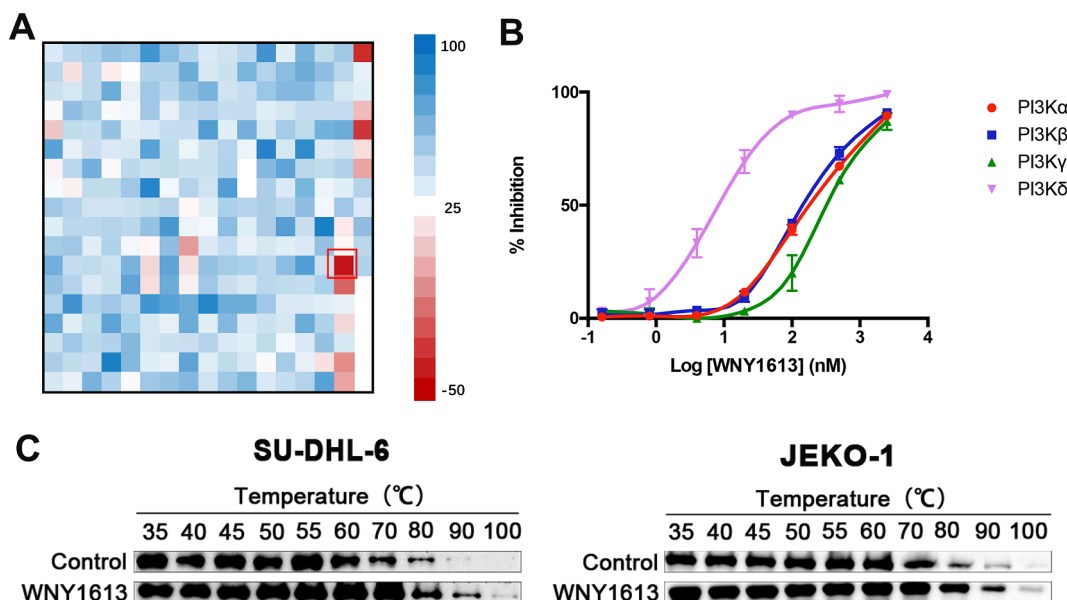


**Fig. 3.** Biochemical characterization of WNY1613. (A) Heat map showing inhibitory rate of WNY1613 against a panel of 300 kinases. The diamond in the red frame represents PI3K $\delta$ . (B) Potency of WNY1613 against PI3K $\alpha$ , PI3K $\beta$ , PI3K $\gamma$  and PI3K $\delta$ . (C) Cellular thermal shift assay from 40°C to 100°C of SU-DHL-6 and JEKO-1 lysates with or without WNY1613 incubation. Data represent the average inhibitory rate of two replicates for (A) and average  $\pm$  SD of three replicates for (B). (For interpretation of the references to colour in this figure legend, the reader is referred to the web version of this article.)

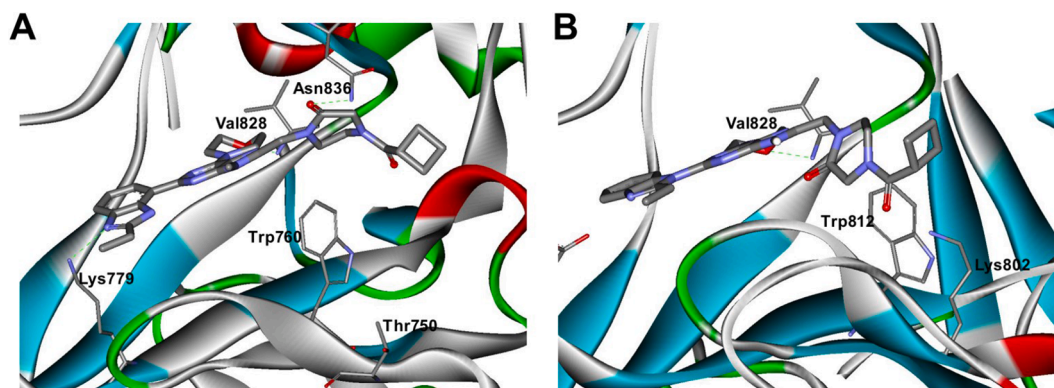


**Fig. 4.** Predicted binding modes of WNY1613 with PI3K $\delta$  (A) and PI3K $\gamma$  (B). Hydrogen bonds are shown as green dashed lines. (For interpretation of the references to colour in this figure legend, the reader is referred to the web version of this article.)

**Table 3**

IC<sub>50</sub> values of Idelalisib and WNY1613 against a panel of NHL cell lines.

Cell lines	Idelalisib (IC <sub>50</sub> : $\mu$ M)	WNY1613 (IC <sub>50</sub> : $\mu$ M)
U2932	>10	>10
OCI-LY-10	>10	>10
OCI-LY-3	5.2 $\pm$ 2.3	1.6 $\pm$ 0.2
DB	>10	>10
SU-DHL-4	0.30 $\pm$ 0.13	0.048 $\pm$ 0.029
WSU-DLCL-2	>10	5.0 $\pm$ 1.7
SU-DHL-6	0.12 $\pm$ 0.03	0.038 $\pm$ 0.011
JEKO-1	0.12 $\pm$ 0.06	0.077 $\pm$ 0.023
Granta-519	1.7 $\pm$ 0.8	0.55 $\pm$ 0.15
NAMALVA	9.2 $\pm$ 2.9	2.0 $\pm$ 0.6

<sup>a</sup> IC<sub>50</sub> values for the antiproliferative activity of Idelalisib and WNY1613 are the mean of three independent measurements and represented as mean  $\pm$  SD.

### 3. Experimental

#### 3.1. Chemistry

Unless otherwise noted, all materials were obtained from commercial suppliers and used without further purification. The <sup>1</sup>H and <sup>13</sup>C NMR spectra were collected on a Bruker Avance 400 spectrometer at 25 °C using CDCl<sub>3</sub> as the solvent. Chemical shifts ( $\delta$ ) are reported in ppm relative to TMS (internal standard), coupling constants (*J*) are reported in hertz, and peak multiplicity are reported as s (singlet), d (doublet), t (triplet), q (quartet), m (multiplet), or br s (broad singlet). Mass spectra (MS) were measured on a Micromass Q-TOF Premier mass spectrometer with electron spray ionization (ESI). Thin layer chromatography (TLC) was performed on 0.20 mm silica gel F-254 plates (Qingdao Haiyang Chemical, China). Preparative thin layer chromatography was performed on 1.00 mm silica gel F-254 plates (Qingdao Haiyang Chemical, China). Visualization of TLC was accomplished with UV light and/or I<sub>2</sub> in silica gel. Column chromatography was performed using silica gel of 300–400 mesh (Qingdao Haiyang Chemical, China). The purities of the title compounds were determined on an UltiMate 3000 (Dionex, USA) HPLC system and were of > 95% purity. (Phenomenex C18 reversed-column, 4.6 mm  $\times$  150 mm, 5  $\mu$ m, isocratic elution with acetonitrile/H<sub>2</sub>O = 60/40 or 65/35; flow rate, 1.0 mL/min; detection wavelength, 254 nm; temperature, 30 °C).

##### 3.1.1. Synthesis of 4-(2-chloro-9-methyl-9H-purin-6-yl)morpholine (2) [26]

Morpholine (150 mmol) was added dropwise to the MeOH (500 mL) solution of 2,6-dichloropurine (18.900 g, 100 mmol) at 0 °C. The mixture was stirred under room temperature for 2 h until the starting materials completely transformed. Then the precipitate was collected by

filtration, and the filter cake was washed by water (50 mL) and MeOH (30 mL), dried under reduced pressure to afford 4-(2-Chloro-9H-purin-6-yl)morpholine (21.412 g, 90%) as a white solid. ESI-MS [M + Na]<sup>+</sup> (*m/z*): 262.2.

Cs<sub>2</sub>CO<sub>3</sub> (24.437 g, 75 mmol) and MeI (4.7 mL, 75 mmol) was slowly added to the acetonitrile solution of 4-(2-Chloro-9H-purin-6-yl)morpholine (11.965 g, 50 mmol). The mixture was stirred under room temperature for 4 h until the starting materials completely transformed. The solvent was removed under reduced pressure and the residue was suspended in dichloromethane. The suspension was stirred for 1 h and separated by filtration. The filtrate was concentrated under reduced pressure to afford the crude product, which was recrystallized by ethyl acetate to afford 4-(2-chloro-9-methyl-9H-purin-6-yl)morpholine (11.633 g, 91%) as a white solid. ESI-MS [M + Na]<sup>+</sup> (*m/z*): 276.1.

##### 3.1.2. Synthesis of (2-chloro-9-methyl-6-morpholino-9H-purin-8-yl)methanol (3) [26]

2.5 M solution of *n*-butyl lithium (9.6 mL, 24 mmol) in *n*-hexane was slowly added to the solution of 2 (5.065 g, 20 mmol) in anhydrous tetrahydrofuran (30 mL) at  $-78$  °C. The resulting mixture was stirred under  $-78$  °C for 1 h and anhydrous dimethylformamide (2.3 mL, 30 mmol) was added, followed by stirring for another 2 h under  $-78$  °C. Then it was warmed up to room temperature and the reaction mixture was poured into cold saturated ammonium chloride solution (100 mL) and stirred for 30 min. After filtration, the filter cake was washed with ice water (20 mL) and dried under vacuum to afford 2-chloro-9-methyl-6-morpholino-9H-purine-8-carbaldehyde as a yellowish solid (5.407 g, 95%). ESI-MS [M+H]<sup>+</sup> (*m/z*): 284.0.

Sodium borohydride (0.756 g, 20 mmol) was slowly added to the suspension of 2-chloro-9-methyl-6-morpholino-9H-purine-8-carbaldehyde (2.830 g, 10 mmol) in MeOH (30 mL) at  $-10$  °C. The resulting mixture was stirred under  $-10$  °C for 1 h until the starting materials completely transformed. Then 90 mL of ice water was added to the reaction mixture and the mixture was stirred for another 10 min. After filtration, the filter cake was washed with ice water (20 mL) and dried under vacuum to afford the product 3 as a white solid (2.625 g, 92%). ESI-MS [M + Na]<sup>+</sup> (*m/z*): 308.1.

##### 3.1.3. Synthesis of (2-(2-ethyl-1H-benzo[d]imidazol-1-yl)-9-methyl-6-morpholino-9H-purin-8-yl)methanol (4) [26]

Under nitrogen atmosphere, a 1,4-dioxane solution of (2-chloro-9-methyl-6-morpholino-9H-purin-8-yl)methanol (3) (2.566 g, 9 mmol), 2-ethyl-1H-benzo[d]imidazole, Pd<sub>2</sub>(dba)<sub>3</sub> (0.9 mmol), Xphos (1.8 mmol) and CsCO<sub>3</sub> (18 mmol) was warmed up to 110 °C and stirred for 5 h until the starting materials completely transformed. The reaction mixture was filtered after cooled to room temperature, and the filtrate was purified by column chromatography with dichloromethane/methanol (V/V = 100/1–50/1) to afford (2-(2-ethyl-1H-benzo[d]imidazol-1-yl)-9-methyl-

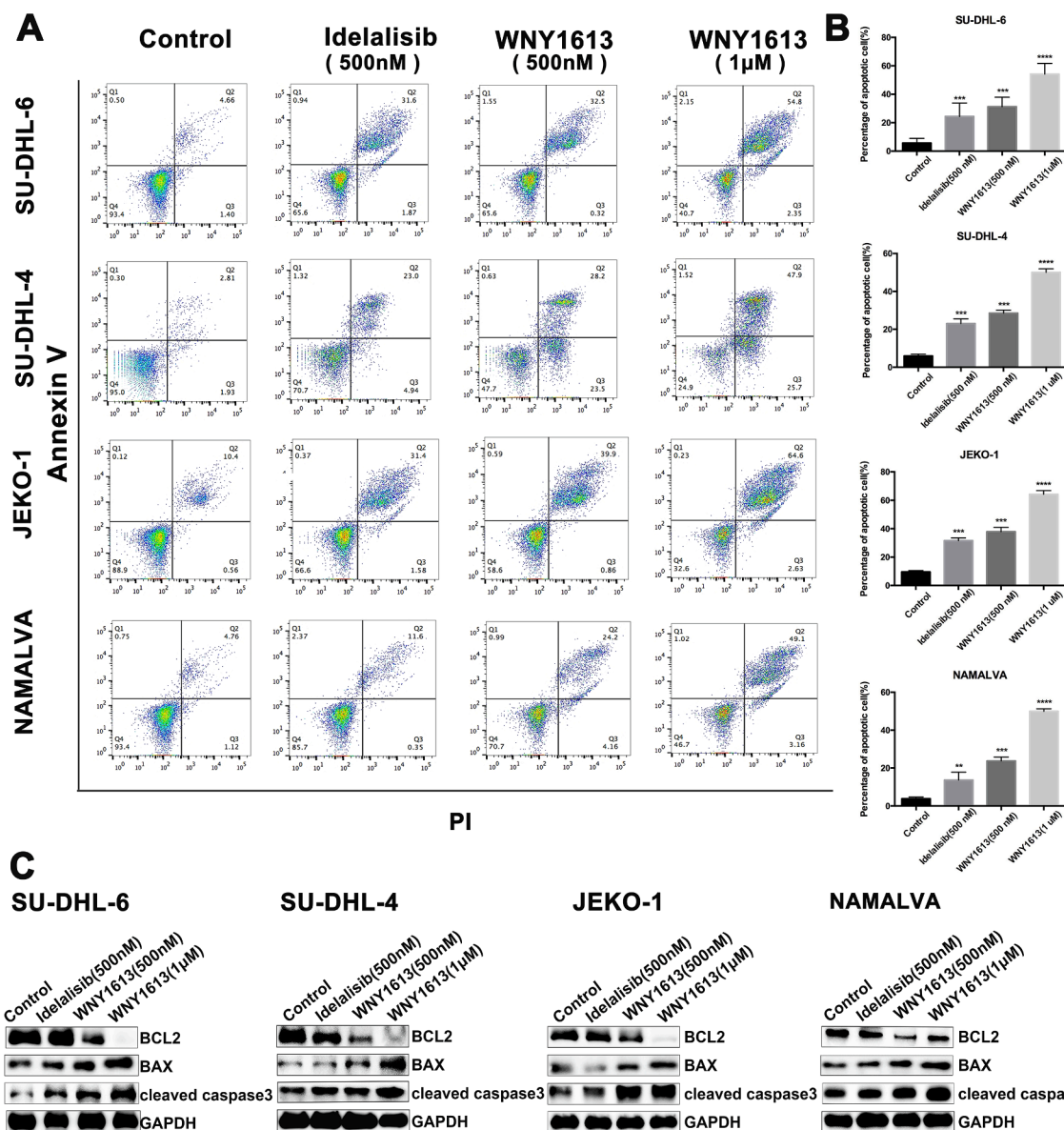


**Fig. 5.** WNY1613 induced cancer cell apoptosis in NHL cell lines. (A) FCM analysis of the apoptosis cells in four NHL cell lines after treatment with Idelalisib and WNY1613 with indicated concentrations for 72 h. (B) Quantification of the FCM analysis. Graphic data were run in triplicate and shown as the mean  $\pm$  SD, \* $p$  < 0.05, \*\* $p$  < 0.01, \*\*\* $p$  < 0.001. (C) Western blotting analysis of apoptosis related protein levels, including BCL2, Bax and cleaved caspase-3, after treated with Idelalisib or WNY1613 with the indicated concentrations for 72 h.

6-morpholino-9H-purin-8-yl)methanol (4) as a yellowish solid (1.874 g, 53%). ESI-MS  $[M + H]^+$  ( $m/z$ ): 396.2.

### 3.1.4. Synthesis of 4-(8-(chloromethyl)-2-(2-ethyl-1H-benzo[d]imidazol-1-yl)-9-methyl-9H-purin-6-yl)morpholine (5) [26]

SOCl<sub>2</sub> (9 mmol) was slowly added to the dichloromethane solution of 4 (1.778 g, 4.5 mmol) at 0 °C over 10 min. The reaction mixture was stirred under room temperature for 2 h until the starting materials completely transformed. After concentrated under reduced pressure, the residue was suspended in water (20 mL) and stirred for 1 h. After filtration, the filter cake was washed by cold water (10 mL) and dried under vacuum to afford 4-(8-(chloromethyl)-2-(2-ethyl-1H-benzo[d]imidazol-1-yl)-9-methyl-9H-purin-6-yl)morpholine (5) as a yellowish solid (1.719 g, 92%). ESI-MS  $[M + H]^+$  ( $m/z$ ): 414.3.

### 3.1.5. Synthesis of 1-((2-(2-ethyl-1H-benzo[d]imidazol-1-yl)-9-methyl-6-morpholino-9H-purin-8-yl)methyl)piperazin-2-one trifluoroacetate (6)

*t*-BuOK (7.5 mmol) was added to the solution of 1-boc-3-

oxopiperazine (1.005 g, 5 mmol) in anhydrous tetrahydrofuran (20 mL). The mixture was stirred for 20 min under room temperature after by compound 5 (1.653 g, 4 mmol) added. Then the reaction mixture was warmed up to room temperature and stirred for another 4 h until the starting materials completely transformed. The solvent was removed under reduced pressure and the residue was extracted with water and ethyl acetate. The organic phase was washed with brine, dried over Na<sub>2</sub>SO<sub>4</sub>, and concentrated under reduced pressure. The crude product was purified by column chromatography with dichloromethane/methanol ( $V/V = 100/1-50/1$ ) as mobile phase to afford *tert*-butyl 4-((2-(2-ethyl-1H-benzo[d]imidazol-1-yl)-9-methyl-6-morpholino-9H-purin-8-yl)methyl)-3-oxopiperazine-1-carboxylate (1.829 g, 79%), which was further deprotected of the boc group with trifluoroacetic acid in dichloromethane to produce 6 with yield of 100%.

### 3.1.6. General procedure for the synthesis of 7a-7d

DIPEA (1.0 mmol) was added to the isopropanol (5 mL) solution of different 1-substituted piperazin-2-ones (0.3 mmol) and 5 (0.083 g, 0.2

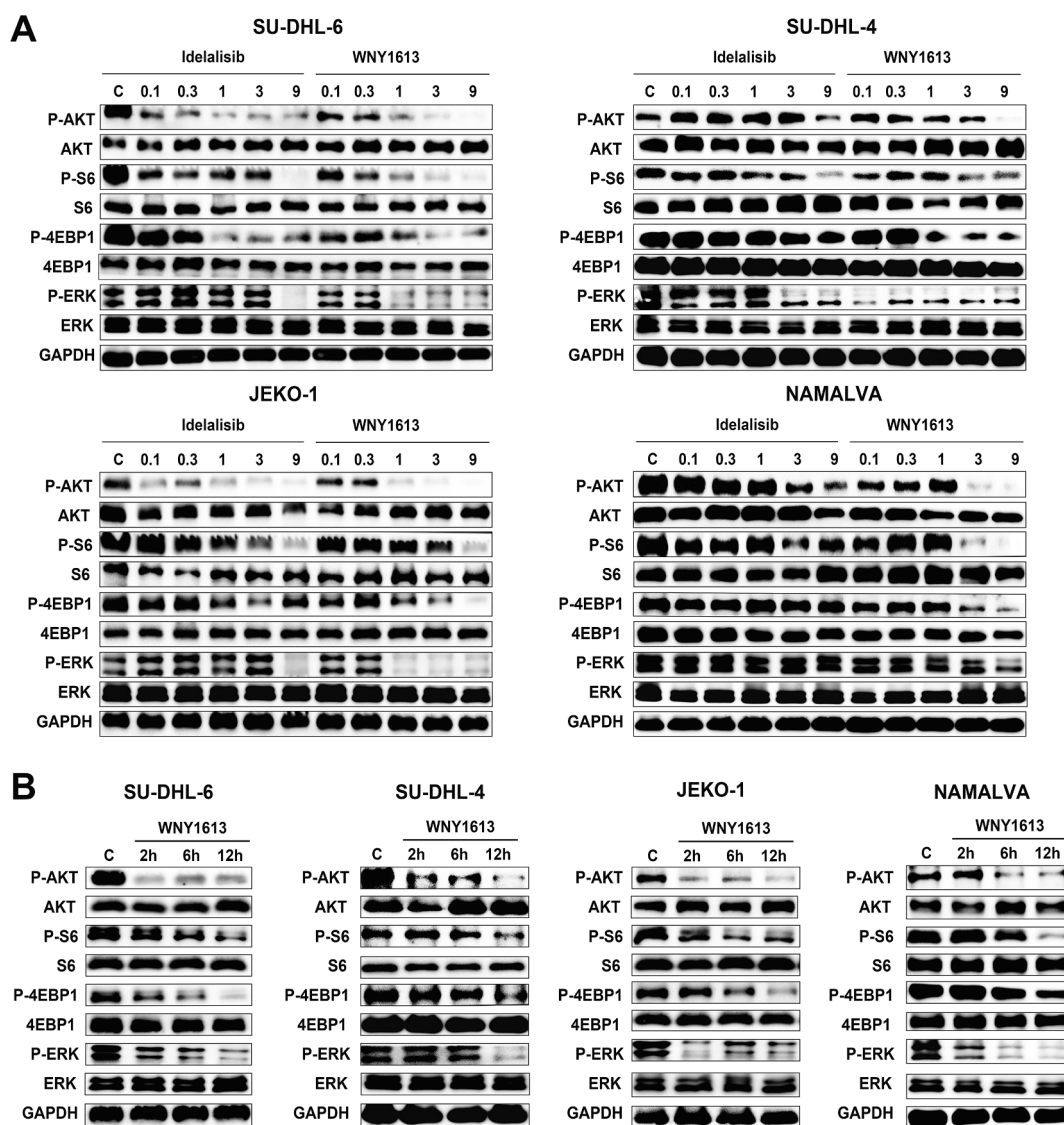


**Fig. 6.** WNY1613 showed a dose- and time-dependent downregulation of PI3K pathway related proteins in all four NHL cell lines. (A) Western blotting analysis for PI3K pathway related proteins, including p-AKT, AKT, p-S6, S6, p-4EBP1, 4EBP1, p-ERK and ERK, after treatment with Idelalisib or WNY1613 with indicated concentrations ( $\mu\text{M}$ ) for 24 h. (B) Western blotting analysis for PI3K pathway related proteins after treatment with Idelalisib or WNY1613 (1  $\mu\text{M}$  for SU-DHL-6 and JEKO-1 cell lines, 3  $\mu\text{M}$  for SU-DHL-4 cell line and 9  $\mu\text{M}$  for NAMALVA cell line) for indicated times.

mmol). The mixture was stirred under  $85^\circ\text{C}$  for 24 h until the starting materials completely transformed. The solvent was removed under reduced pressure and the residue was extracted with water/dichloromethane, the organic phase was washed with brine and dried over  $\text{MgSO}_4$ . The crude product was purified by preparative TLC with dichloromethane/methanol (V/V = 10/1) as mobile phase to afford the title compounds **7a-7d** with yields of 40%-70%.

**1-(cyclopropylmethyl)-4-((2-(2-ethyl-1H-benzo[d]imidazol-1-yl)-9-methyl-6-morpholino-9H-purin-8-yl)methyl)piperazin-2-one (7a).** White solid, yield: 68%.  $^1\text{H}$  NMR (400 MHz,  $\text{CDCl}_3$ )  $\delta$  8.11–7.97 (m, 1H), 7.87–7.72 (m, 1H), 7.41–7.22 (m, 2H), 4.36 (s br, 4H), 3.89 (d,  $J = 6.8$  Hz, 6H), 3.84 (s, 3H), 3.45 (t,  $J = 5.6$  Hz, 2H), 3.37 (q,  $J = 7.5$  Hz, 2H), 3.31 (d,  $J = 8.9$  Hz, 4H), 2.84 (t,  $J = 5.6$  Hz, 2H), 1.46 (t,  $J = 7.5$  Hz, 3H), 0.98 (d,  $J = 6.9$  Hz, 1H), 0.54 (d,  $J = 7.6$  Hz, 2H), 0.26 (d,  $J = 5.1$  Hz, 2H).  $^{13}\text{C}$  NMR (101 MHz,  $\text{CDCl}_3$ )  $\delta$  166.02, 156.93, 153.69 (2C), 150.69, 146.62, 142.49, 134.58, 122.84, 122.67, 119.04, 117.00, 113.22, 67.01 (2C), 57.35, 54.23, 50.50, 49.49, 46.40 (2C), 45.68, 29.21, 23.74, 12.39, 8.96, 3.55 (2C). ESI-MS  $[\text{M}+\text{H}]^+$  ( $m/z$ ): 530.3.

**1-cyclopentyl-4-((2-(2-ethyl-1H-benzo[d]imidazol-1-yl)-9-methyl-6-morpholino-9H-purin-8-yl)methyl)piperazin-2-one (7b).** White solid, yield:

62%.  $^1\text{H}$  NMR (400 MHz,  $\text{CDCl}_3$ )  $\delta$  8.05–7.94 (m, 1H), 7.75 (dd,  $J = 5.7$ , 3.3 Hz, 1H), 7.33–7.19 (m, 2H), 5.03–4.83 (m, 2H), 3.89–3.70 (m, 9H), 3.65–3.56 (m, 1H), 3.50 (d,  $J = 5.4$  Hz, 1H), 3.42–3.12 (m, 7H), 2.86–2.71 (m, 2H), 1.92–1.76 (m, 4H), 1.74–1.57 (m, 4H), 1.45 (t,  $J = 7.5$  Hz, 3H).  $^{13}\text{C}$  NMR (101 MHz,  $\text{CDCl}_3$ )  $\delta$  166.14, 156.94, 153.70 (2C), 150.73, 146.61, 142.60, 134.62, 122.73, 122.65, 119.10, 116.99, 113.23, 67.02 (2C), 57.60, 54.22, 53.85, 49.66 (2C), 45.89, 40.92, 29.20, 27.87 (2C), 24.07 (2C), 23.77, 12.38. ESI-MS  $[\text{M}+\text{H}]^+$  ( $m/z$ ): 544.3.

**4-((2-(2-ethyl-1H-benzo[d]imidazol-1-yl)-9-methyl-6-morpholino-9H-purin-8-yl)methyl)-1-(1-methyl-1H-pyrazol-4-yl)piperazin-2-one (7c).** Pale solid, yield: 69%.  $^1\text{H}$  NMR (400 MHz,  $\text{CDCl}_3$ )  $\delta$  8.03 (s, 1H), 8.02–7.97 (m, 1H), 7.80–7.71 (m, 1H), 7.46 (s, 1H), 7.34–7.22 (m, 2H), 4.36 (s, 4H), 4.01–3.77 (m, 12H), 3.71 (t,  $J = 5.5$  Hz, 2H), 3.43 (s, 2H), 3.35 (q,  $J = 7.5$  Hz, 2H), 2.96 (t,  $J = 5.5$  Hz, 2H), 1.45 (t,  $J = 7.5$  Hz, 3H).  $^{13}\text{C}$  NMR (101 MHz,  $\text{CDCl}_3$ )  $\delta$  164.10, 156.93, 153.72 (2C), 150.78, 146.31, 142.56, 134.59, 129.45, 124.84, 123.08, 122.84, 122.68, 119.08, 117.01, 113.22, 67.01 (2C), 57.76, 54.11, 49.10, 47.44 (2C), 45.89, 39.34, 29.22, 23.78, 12.38. ESI-MS  $[\text{M}+\text{H}]^+$  ( $m/z$ ): 556.3.

**2-(4-((2-(2-ethyl-1H-benzo[d]imidazol-1-yl)-9-methyl-6-morpholino-**

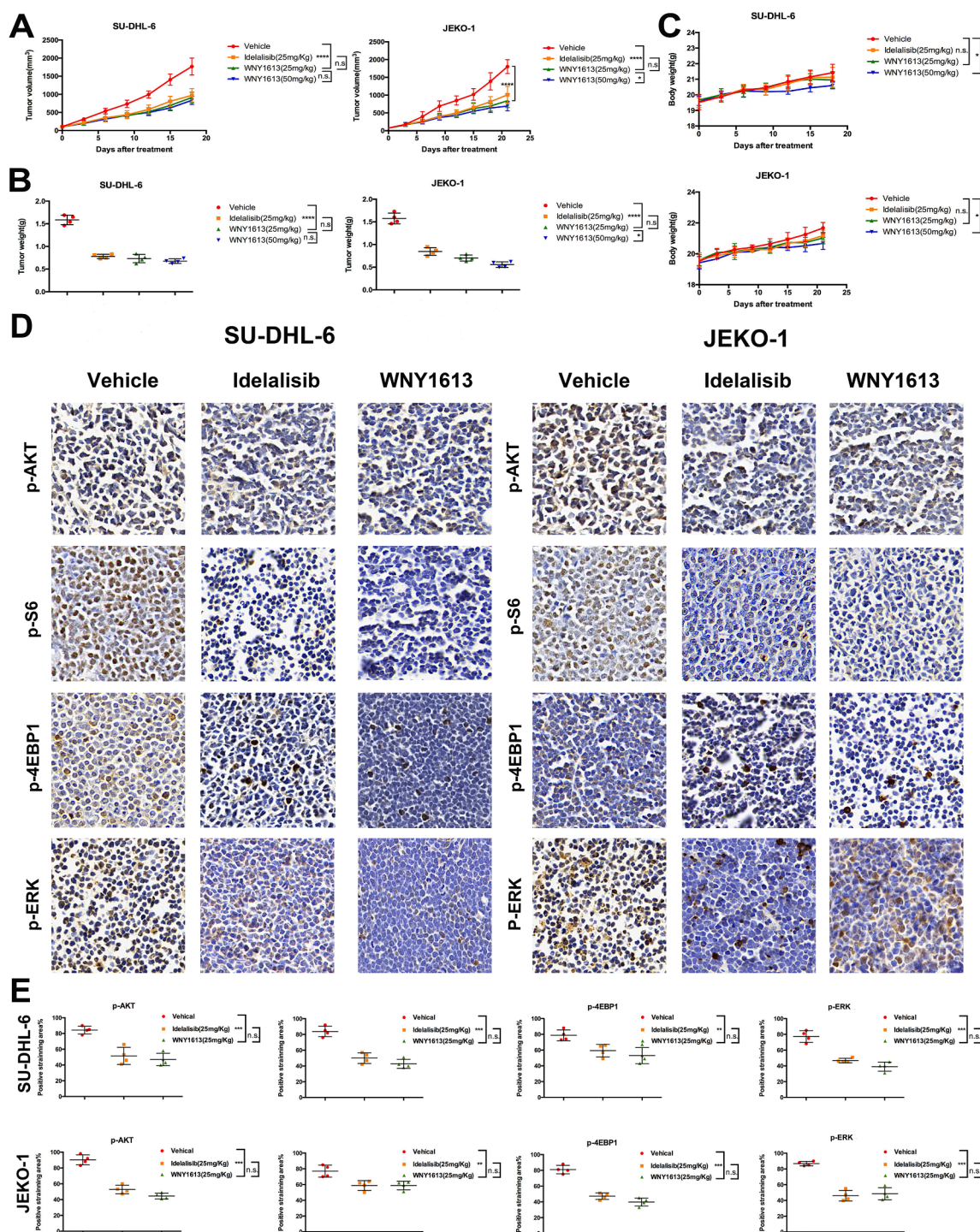


**Fig. 7.** In vivo anticancer activity of WNY1613 in NHL xenograft models. Tumor bearing NOD-SCID mice were orally treated with vehicle, Idelalisib (25 mg/kg), WNY1613(25 mg/kg) and WNY1613(50 mg/kg) once every day for indicated days. (A) Volume of tumors from sacrificed mice, data are presented as the mean ± SD. (B) Weight of tumors from sacrificed mice, data are presented as the mean ± SD. (C) The average body weight changes of the vehicle, Idelalisib, WNY1613 treated groups, data are presented as the mean ± SD. (D) Immunohistochemical analysis of p-AKT, p-S6, p-4EBP1 and p-ERK levels in tumor tissues of SU-DHL-6 and JEKO-1 xenograft models from sacrificed mice. (E) Quantification of percentage of positive staining cells, data are presented as the mean ± SD, \*p < 0.05, \*\*p < 0.01, \*\*\*p < 0.001, \*\*\*\*p < 0.0001.

*9H-purin-8-yl)methyl)-2-oxopiperazin-1-yl)acetamide (7d)*. Yellowish solid, yield: 43%. <sup>1</sup>H NMR (400 MHz, CDCl<sub>3</sub>) δ 8.08–7.96 (m, 1H), 7.82–7.69 (m, 1H), 7.27 (q, J = 3.7 Hz, 2H), 6.27 (s, 1H), 5.56 (s, 1H), 4.35 (s br, 4H), 4.03 (s, 2H), 3.99–3.80 (m, 9H), 3.50 (t, J = 5.5 Hz, 2H), 3.35 (q, J = 7.7 Hz, 2H), 3.34 (s, 2H), 2.88 (t, J = 5.5 Hz, 2H), 1.45 (t, J = 7.5, 3H). <sup>13</sup>C NMR (101 MHz, CDCl<sub>3</sub>) δ 170.22, 167.32, 156.93, 153.72, 153.67, 150.76, 146.28, 142.50, 134.57, 122.86, 122.70,

119.06, 117.00, 113.22, 67.00 (2C), 57.03, 54.01, 50.39, 49.33, 48.05 (2C), 45.79, 29.21, 23.75, 12.38. ESI-MS [M+H]<sup>+</sup> (m/z): 533.3.

### 3.1.7. Synthesis of 1-((2-(2-ethyl-1H-benzo[d]imidazol-1-yl)-9-methyl-6-morpholino-9H-purin-8-yl)methyl)-4-(2,2,2-trifluoroethyl)piperazin-2-one (8a)

2,2,2-Trifluoroethyl methanesulfonate (0.3 mmol) and K<sub>2</sub>CO<sub>3</sub> (0.3

mmol) were added to the acetonitrile solution of **6** (0.089 g, 0.15 mmol). The mixture was stirred under 85 °C for 2 h until the starting materials completely transformed. The solvent was removed under reduced pressure and the residue was extracted with water and ethyl acetate. The organic phase was washed with brine, dried over Na<sub>2</sub>SO<sub>4</sub>, and concentrated under reduced pressure. The crude product was purified by preparative TLC with dichloromethane/methanol (V/V = 10/1) as mobile phase to afford **8a** (0.042 g, 50%) as a white solid. <sup>1</sup>H NMR (400 MHz, CDCl<sub>3</sub>) δ 8.07–7.95 (m, 1H), 7.82–7.70 (m, 1H), 7.33–7.21 (m, 2H), 4.87 (s, 2H), 4.35 (s br, 4H), 3.86 (t, *J* = 7.2 Hz, 4H), 3.84 (s, 3H), 3.50 (t, *J* = 5.8 Hz, 2H), 3.48 (s, 2H), 3.35 (q, *J* = 7.5 Hz, 2H), 3.08 (q, *J* = 9.2 Hz, 2H), 2.97 (t, *J* = 5.4 Hz, 2H), 1.44 (t, *J* = 7.5 Hz, 3H). <sup>13</sup>C NMR (101 MHz, CDCl<sub>3</sub>) δ 166.02, 156.91, 153.68, 153.46, 150.83, 145.96, 142.48, 134.54, 124.90 (q, *J* = 279 Hz), 122.89, 122.72, 119.08, 117.27, 113.23, 66.99 (2C), 57.18, 57.04 (q, *J* = 29 Hz), 50.03, 46.48 (2C), 45.89, 42.03, 29.25, 23.78, 12.37. <sup>19</sup>F NMR (376 MHz, CDCl<sub>3</sub>) δ –69.17. ESI-MS [M + H]<sup>+</sup> (*m/z*): 558.2

### 3.1.8. General procedure for the synthesis of **8b–8i**.

Sodium acetate (0.3 mmol) and sodium triacetoxyborohydride (0.4 mmol) was added to the dichloromethane (10 mL) solution of **6** (0.089 g, 0.15 mmol) and different aldehydes or ketones (0.25 mmol) at 0 °C. The mixture was stirred under room temperature for 12 h until the starting materials completely transformed. Then saturated sodium bicarbonate solution was added to the reaction mixture and the mixture was stirred for another 30 min. After the organic phase separated by extraction, the aqueous phase was reextracted with dichloromethane. The combined organic phase was washed with brine, dried over MgSO<sub>4</sub> and concentrated under reduced pressure. The crude product was further purified by preparative TLC with dichloromethane/methanol (V/V = 10/1) to afford **8b–8i** with yields of 30–60%.

4-cyclopentyl-1-((2-(2-ethyl-1H-benzo[d]imidazol-1-yl)-9-methyl-6-morpholino-9H-purin-8-yl)methyl)piperazin-2-one (**8b**). White solid, yield: 54%. <sup>1</sup>H NMR (400 MHz, CDCl<sub>3</sub>) δ 8.07–7.93 (m, 1H), 7.84–7.68 (m, 1H), 7.32–7.19 (m, 2H), 4.87 (s, 2H), 4.48–4.19 (s br, 4H), 3.92–3.79 (m, 7H), 3.49–3.24 (m, 6H), 2.75 (q, *J* = 5.4, 2H), 2.57 (t, *J* = 7.6 Hz, 1H), 1.98–1.78 (m, 2H), 1.78–1.65 (m, 2H), 1.63–1.51 (m, 2H), 1.50–1.35 (m, 5H). <sup>13</sup>C NMR (101 MHz, CDCl<sub>3</sub>) δ 167.15, 156.95, 153.67, 153.49, 150.78, 146.24, 142.47, 134.55, 122.89, 122.72, 119.08, 117.27, 113.24, 67.02 (2C), 66.60, 56.77, 48.66, 46.52 (2C), 45.89, 41.89, 30.37 (2C), 29.33, 24.05 (2C), 23.77, 12.39. ESI-MS [M + H]<sup>+</sup> (*m/z*): 544.3.

4-cyclohexyl-1-((2-(2-ethyl-1H-benzo[d]imidazol-1-yl)-9-methyl-6-morpholino-9H-purin-8-yl)methyl)piperazin-2-one (**8c**). White solid, yield: 59%. <sup>1</sup>H NMR (400 MHz, CDCl<sub>3</sub>) δ 8.04–7.96 (m, 1H), 7.80–7.72 (m, 1H), 7.32–7.22 (m, 2H), 4.87 (s, 2H), 4.30 (s br, 4H), 3.95–3.78 (m, 7H), 3.45–3.28 (m, 6H), 2.76 (q, *J* = 5.4, 2H), 2.32 (dd, *J* = 13.5, 6.1 Hz, 1H), 1.95–1.78 (m, 4H), 1.44 (t, *J* = 7.5 Hz, 3H), 1.35–1.05 (m, 6H). <sup>13</sup>C NMR (101 MHz, CDCl<sub>3</sub>) δ 167.66, 156.93, 153.58, 153.49, 150.74, 146.34, 142.39, 134.53, 122.91, 122.74, 119.05, 117.27, 113.25, 67.02 (2C), 62.36, 53.67, 46.86, 45.90 (3C), 41.98, 29.31, 28.60 (2C), 26.04, 25.43 (2C), 23.75, 12.39. ESI-MS [M + H]<sup>+</sup> (*m/z*): 558.3.

4-(4,4-difluorocyclohexyl)-1-((2-(2-ethyl-1H-benzo[d]imidazol-1-yl)-9-methyl-6-morpholino-9H-purin-8-yl)methyl)piperazin-2-one (**8d**). White solid, yield: 43%. <sup>1</sup>H NMR (400 MHz, CDCl<sub>3</sub>) δ 8.09–7.96 (m, 1H), 7.82–7.70 (m, 1H), 7.33–7.20 (m, 2H), 4.87 (s, 2H), 4.35 (s br, 4H), 3.99–3.78 (m, 7H), 3.43 (dd, *J* = 6.3, 4.4 Hz, 2H), 3.40–3.27 (m, 4H), 2.77 (t, *J* = 5.3 Hz, 2H), 2.42 (d, *J* = 9.7 Hz, 1H), 2.25–2.04 (m, 2H), 1.91–1.58 (m, 6H), 1.44 (t, *J* = 7.4 Hz, 3H). <sup>13</sup>C NMR (101 MHz, CDCl<sub>3</sub>) δ 167.12, 156.92, 153.67, 153.45, 150.79, 146.16, 142.48, 134.54, 122.87, 122.70, 122.68 (t, *J* = 239 Hz), 119.05, 117.26, 113.24, 66.99 (2C), 59.42, 54.17, 46.83, 45.96 (3C), 41.97, 31.86 (t, *J* = 24.5 Hz, 2C), 29.27, 24.35 (2C), 23.78, 12.38. ESI-MS [M + H]<sup>+</sup> (*m/z*): 594.3.

1-((2-(2-ethyl-1H-benzo[d]imidazol-1-yl)-9-methyl-6-morpholino-9H-purin-8-yl)methyl)-4-(1-methylpiperidin-4-yl)piperazin-2-one (**8e**). White solid, yield: 39%. <sup>1</sup>H NMR (400 MHz, CDCl<sub>3</sub>) δ 8.01 (d, *J* = 4.7 Hz, 1H),

7.74 (d, *J* = 4.5 Hz, 1H), 7.27 (dd, *J* = 8.8, 5.3 Hz, 2H), 4.86 (s, 2H), 3.95–3.75 (m, 7H), 3.44 (d, *J* = 13.1 Hz, 4H), 3.33 (d, *J* = 12.5 Hz, 4H), 3.00 (d, *J* = 10.9 Hz, 2H), 2.77 (q, *J* = 5.4, 2H), 2.35 (s, 5H), 2.12 (t, *J* = 10.3 Hz, 3H), 1.84 (d, *J* = 9.8 Hz, 2H), 1.68 (dd, *J* = 30.0, 19.6 Hz, 2H), 1.41 (t, *J* = 7.5 Hz, 3H). <sup>13</sup>C NMR (101 MHz, CDCl<sub>3</sub>) δ 167.27, 156.94, 153.65, 153.43, 150.73, 146.20, 142.43, 134.52, 122.89, 122.79, 119.00, 117.26, 113.24, 66.99 (2C), 59.41, 54.42 (2C), 54.15, 46.79, 45.90, 45.53 (2C), 45.49, 41.94, 29.27, 27.28 (2C), 23.73, 12.38. ESI-MS [M + H]<sup>+</sup> (*m/z*): 573.3.

1-((2-(2-ethyl-1H-benzo[d]imidazol-1-yl)-9-methyl-6-morpholino-9H-purin-8-yl)methyl)-4-(tetrahydro-2H-pyran-4-yl)piperazin-2-one (**8f**). White solid, yield: 45%. <sup>1</sup>H NMR (400 MHz, CDCl<sub>3</sub>) δ 8.07–7.94 (m, 1H), 7.83–7.70 (m, 1H), 7.37–7.20 (m, 2H), 4.87 (s, 2H), 4.31 (s br, 4H), 4.03 (dd, *J* = 11.5, 2.9 Hz, 2H), 3.95–3.76 (m, 7H), 3.53–3.29 (m, 8H), 2.79 (q, *J* = 5.4, 2H), 2.48 (m, 1H), 1.91–1.70 (m, 2H), 1.55 (m, 2H), 1.44 (t, *J* = 7.5 Hz, 3H). <sup>13</sup>C NMR (101 MHz, CDCl<sub>3</sub>) δ 167.21, 156.92, 153.66, 153.45, 150.72, 146.21, 142.25, 134.47, 122.95, 122.87, 118.98, 117.28, 113.26, 66.99 (4C), 59.68 (2C), 53.83, 46.73, 45.89, 45.57 (2C), 41.96, 29.30, 29.24 (2C), 23.71, 12.39. ESI-MS [M + H]<sup>+</sup> (*m/z*): 560.3.

1-((2-(2-ethyl-1H-benzo[d]imidazol-1-yl)-9-methyl-6-morpholino-9H-purin-8-yl)methyl)-4-(tetrahydro-2H-thiopyran-4-yl)piperazin-2-one (**8g**). White solid, yield: 51%. <sup>1</sup>H NMR (400 MHz, CDCl<sub>3</sub>) δ 8.00 (d, *J* = 6.8 Hz, 1H), 7.76 (d, *J* = 6.6 Hz, 1H), 7.32 (d, *J* = 32.2 Hz, 2H), 4.87 (s, 2H), 4.35 (s br, 4H), 3.95–3.75 (m, 7H), 3.45–3.30 (m, 6H), 2.80–2.57 (m, 6H), 2.47–2.32 (m, 1H), 2.21–2.02 (m, 2H), 1.72–1.64 (m, 2H), 1.44 (t, *J* = 7.5 Hz, 3H). <sup>13</sup>C NMR (101 MHz, CDCl<sub>3</sub>) δ 167.44, 156.90, 153.66, 153.44, 150.65, 146.29, 142.00, 134.40, 122.94, 122.86, 118.92, 117.31, 113.28, 67.00 (2C), 61.39, 53.23, 46.95, 45.64, 45.43 (2C), 42.01, 29.93 (2C), 29.29, 28.34 (2C), 23.65, 12.42. ESI-MS [M + H]<sup>+</sup> (*m/z*): 576.3.

4-(1,1-dioxidotetrahydro-2H-thiopyran-4-yl)-1-((2-(2-ethyl-1H-benzo[d]imidazol-1-yl)-9-methyl-6-morpholino-9H-purin-8-yl)methyl)piperazin-2-one (**8h**). White solid, yield: 33%. <sup>1</sup>H NMR (400 MHz, CDCl<sub>3</sub>) δ 8.06–7.96 (m, 1H), 7.81–7.70 (m, 1H), 7.33–7.20 (m, 2H), 4.87 (s, 2H), 4.35 (s br, 4H), 3.99–3.78 (m, 7H), 3.48 (dd, *J* = 6.3, 4.4 Hz, 2H), 3.41–3.29 (m, 4H), 3.27–3.12 (m, 2H), 2.99–2.86 (m, 2H), 2.78 (t, *J* = 6.3 Hz, 2H), 2.58 (d, *J* = 3.2 Hz, 1H), 2.33–2.12 (m, 4H), 1.44 (t, *J* = 7.4 Hz, 3H). <sup>13</sup>C NMR (101 MHz, CDCl<sub>3</sub>) δ 166.30, 156.90, 153.70, 153.44, 150.87, 145.89, 142.50, 134.54, 122.89, 122.73, 119.10, 117.30, 113.25, 66.99 (2C), 57.10, 54.27, 48.64 (2C), 46.63, 45.75 (3C), 41.92, 29.30, 25.80 (2C), 23.81, 12.38. ESI-MS [M + H]<sup>+</sup> (*m/z*): 608.3.

1-((2-(2-ethyl-1H-benzo[d]imidazol-1-yl)-9-methyl-6-morpholino-9H-purin-8-yl)methyl)-4-(1,4-dioxaspiro[4.5]decan-8-yl)piperazin-2-one (**8i**). **8i** was prepared from **6** (0.3 mmol) as a white solid, yield: 57%. <sup>1</sup>H NMR (400 MHz, CDCl<sub>3</sub>) δ 8.00 (d, *J* = 5.4 Hz, 1H), 7.82–7.69 (m, 1H), 7.26 (d, *J* = 4.9 Hz, 2H), 4.86 (s, 2H), 4.35 (s br, 4H), 3.93 (s br, 4H), 3.87 (s, 4H), 3.83 (s, 3H), 3.46–3.24 (m, 6H), 2.77 (q, *J* = 5.4, 2H), 2.45–2.35 (m, 1H), 1.88–1.49 (m, 8H), 1.44 (t, *J* = 7.5, 3H). <sup>13</sup>C NMR (101 MHz, CDCl<sub>3</sub>) δ 167.55, 156.92, 153.66, 153.47, 150.74, 146.29, 142.45, 134.54, 122.87, 122.70, 119.04, 117.27, 113.24, 108.17, 67.00 (2C), 64.37, 64.29, 60.51, 54.12, 46.95, 45.91 (3C), 41.99, 33.18 (2C), 29.28, 25.36 (2C), 23.76, 12.38. ESI-MS [M + H]<sup>+</sup> (*m/z*): 616.3.

### 3.1.9. Synthesis of 1-((2-(2-ethyl-1H-benzo[d]imidazol-1-yl)-9-methyl-6-morpholino-9H-purin-8-yl)methyl)-4-(4-oxocyclohexyl)piperazin-2-one (**8j**)

THF (10 mL) and concentrated hydrochloric acid (2 mL) was added to a solution of **8i** (0.092 g, 0.15 mmol) in dichloromethane (10 mL) under 0 °C. The mixture was stirred under refluxing for 4 h. The solvent was removed under reduced pressure and the residue was dissolved in dichloromethane and purified by preparative TLC with dichloromethane/methanol (V/V = 10/1) as mobile phase to afford **8j** (0.069 g, 80%) as a pale solid. <sup>1</sup>H NMR (400 MHz, CDCl<sub>3</sub>) δ 8.07–7.95 (m, 1H), 7.82–7.69 (m, 1H), 7.27 (q, *J* = 2.2 Hz, 2H), 4.88 (s, 2H), 4.35 (s br, 4H), 3.94–3.78 (m, 7H), 3.47 (t, *J* = 6.3 Hz, 2H), 3.43–3.27 (m, 4H), 2.82 (t, *J* = 6.3 Hz, 2H), 2.77–2.67 (m, 1H), 2.55–2.45 (m, 2H), 2.38–2.27 (m,

2H), 2.14–1.98 (m, 2H), 1.94–1.82 (m, 2H), 1.44 (t,  $J = 7.5$  Hz, 3H).  $^{13}\text{C}$  NMR (101 MHz,  $\text{CDCl}_3$ )  $\delta$  209.89, 166.97, 156.91, 153.68, 153.48, 150.84, 146.10, 142.52, 134.55, 122.87, 122.72, 119.11, 117.27, 113.23, 67.00 (2C), 59.03, 54.37, 46.76, 46.20 (2C), 45.80, 41.95, 38.43 (2C), 29.29, 27.74 (2C), 23.80, 12.38. ESI-MS  $[\text{M} + \text{H}]^+$  ( $m/z$ ): 572.3.

### 3.1.10. Synthesis of 1-((2-(2-ethyl-1H-benzo[d]imidazol-1-yl)-9-methyl-6-morpholino-9H-purin-8-yl)methyl)-4-(4-hydroxycyclohexyl)piperazin-2-one (8k)

Sodium borohydride (0.2 mmol) was slowly added to the suspension of **8 l** (0.052 g, 0.09 mmol) in MeOH (5 mL) at 0 °C. The resulting mixture was stirred under room temperature for 2 h until the starting materials completely transformed. Then the solvent was removed under reduced pressure and the residue was dissolved in dichloromethane and purified by preparative TLC with dichloromethane/methanol ( $V/V = 10/1$ ) as mobile phase to afford **8k** (0.039 g, 76%) as a pale solid.  $^1\text{H}$  NMR (400 MHz,  $\text{CDCl}_3$ )  $\delta$  8.09–7.94 (m, 1H), 7.84–7.69 (m, 1H), 7.41–7.18 (m, 2H), 4.87 (d,  $J = 3.3$  Hz, 2H), 4.35 (s br, 4H), 3.92–3.73 (m, 7H), 3.66–3.52 (m, 1H), 3.52–3.23 (m, 6H), 2.77 (t,  $J = 5.5$  Hz, 2H), 2.42–2.26 (m, 1H), 2.16–1.96 (m, 2H), 1.96–1.50 (m, 4H), 1.44 (t,  $J = 7.4$  Hz, 3H), 1.37–1.21 (m, 2H).  $^{13}\text{C}$  NMR (101 MHz,  $\text{CDCl}_3$ )  $\delta$  167.42, 156.92, 153.66, 153.48, 150.79, 146.25, 142.52, 134.56, 122.86, 122.70, 119.08, 117.26, 113.22, 70.09, 67.01 (2C), 61.35, 53.96, 46.87, 46.25 (2C), 45.77, 41.97, 34.08 (2C), 29.29, 26.25 (2C), 23.78, 12.38. ESI-MS  $[\text{M} + \text{H}]^+$  ( $m/z$ ): 574.3.

### 3.1.11. Synthesis of (S)-1-((2-(2-ethyl-1H-benzo[d]imidazol-1-yl)-9-methyl-6-morpholino-9H-purin-8-yl)methyl)-4-(2-hydroxypropanoyl)piperazin-2-one (8l)

Triethylamine (0.3 mmol), HOBT (0.25 mmol) and EDCI (0.3 mmol) was added to the dichloromethane (5 mL) solution of **6** (0.089 g, 0.15 mmol) and L-lactic acid (0.3 mmol). The mixture was stirred under room temperature for 12 h. Then the mixture was extracted with dichloromethane/water. The organic phase was washed with brine, dried over  $\text{MgSO}_4$  and concentrated under reduced pressure. The crude product was further purified by preparative TLC with dichloromethane/methanol ( $V/V = 10/1$ ) to afford **8l** (0.053 g, 65%) as a white solid.  $^1\text{H}$  NMR (400 MHz,  $\text{CDCl}_3$ )  $\delta$  8.06–7.95 (m, 1H), 7.80–7.71 (m, 1H), 7.27 (q,  $J = 3.9$  Hz, 2H), 4.87 (s, 2H), 4.51–4.09 (m, 8H), 3.92–3.72 (m, 7H), 3.79–3.55 (m, 4H), 3.34 (q,  $J = 7.5$  Hz, 2H), 1.44 (t,  $J = 7.4$  Hz, 3H), 1.36 (d,  $J = 6.7$  Hz, 3H).  $^{13}\text{C}$  NMR (101 MHz,  $\text{CDCl}_3$ )  $\delta$  169.49, 165.01, 156.91, 153.70, 153.40, 150.93, 145.41, 142.47, 134.50, 122.92, 122.77, 119.08, 117.28, 113.22, 66.96 (2C), 64.51, 48.39, 46.03, 45.84 (2C), 42.49, 39.72, 29.26, 23.79, 21.06, 12.37. ESI-MS  $[\text{M} + \text{H}]^+$  ( $m/z$ ): 548.3.

### 3.1.12. General procedure for the synthesis of 8m–8t

Different acyl chloride or sulfonyl chloride (0.3 mmol) was slowly added to the dichloromethane (5 mL) solution of **6** (0.089 g, 0.15 mmol) and triethylamine (0.3 mmol) at 0 °C. The mixture was stirred under room temperature for 3–12 h until the starting materials completely transformed. Then the mixture was extracted with dichloromethane/water. The organic phase was washed with brine, dried over  $\text{MgSO}_4$  and concentrated under reduced pressure. The crude product was further purified by preparative TLC with dichloromethane/methanol ( $V/V = 10/1$ ) to afford **8 m–8 t** with yields of 40%–70%.

4-acetyl-1-((2-(2-ethyl-1H-benzo[d]imidazol-1-yl)-9-methyl-6-morpholino-9H-purin-8-yl)methyl)piperazin-2-one (**8m**). White solid, yield: 62%.  $^1\text{H}$  NMR (400 MHz,  $\text{CDCl}_3$ )  $\delta$  8.06–7.95 (m, 1H), 7.81–7.70 (m, 1H), 7.33–7.22 (m, 2H), 4.88 (d,  $J = 4.6$  Hz, 2H), 4.33 (s br, 6H), 3.92–3.72 (m, 9H), 3.63–3.53 (m, 2H), 3.34 (q,  $J = 7.5$  Hz, 2H), 2.13 (s, 3H), 1.44 (t,  $J = 7.5$  Hz, 3H).  $^{13}\text{C}$  NMR (101 MHz,  $\text{CDCl}_3$ )  $\delta$  168.91, 165.64, 164.68, 156.91, 153.70, 150.91, 145.53, 142.52, 134.53, 122.90, 122.74, 119.10, 117.29, 113.22, 66.97 (2C), 49.68, 46.39, 46.05 (2C), 42.46, 38.54, 29.23, 23.80, 21.34, 12.37. ESI-MS  $[\text{M} + \text{H}]^+$  ( $m/z$ ): 518.3.

1-((2-(2-ethyl-1H-benzo[d]imidazol-1-yl)-9-methyl-6-morpholino-9H-

purin-8-yl)methyl)-4-isobutyrylpiperazin-2-one (**8n**). White solid, yield: 54%.  $^1\text{H}$  NMR (400 MHz,  $\text{CDCl}_3$ )  $\delta$  8.05–7.95 (m, 1H), 7.82–7.73 (m, 1H), 7.27 (q,  $J = 4.7$  Hz, 2H), 4.88 (s, 2H), 4.30 (s br, 6H), 3.92–3.72 (m, 9H), 3.56 (s br, 2H), 3.35 (q,  $J = 7.5$  Hz, 2H), 2.82–2.69 (m, 1H), 1.44 (t,  $J = 7.5$  Hz, 3H), 1.15 (d,  $J = 6.8$  Hz, 6H).  $^{13}\text{C}$  NMR (101 MHz,  $\text{CDCl}_3$ )  $\delta$  170.08, 165.96, 156.89, 153.68, 153.40, 150.82, 145.09, 142.20, 134.44, 122.98, 122.83, 119.01, 117.31, 113.23, 66.97 (2C), 49.11, 46.45, 46.13 (2C), 42.43, 38.86, 30.55, 29.24, 23.70, 19.17 (2C), 12.38. ESI-MS  $[\text{M} + \text{H}]^+$  ( $m/z$ ): 546.3.

4-(cyclopropanecarbonyl)-1-((2-(2-ethyl-1H-benzo[d]imidazol-1-yl)-9-methyl-6-morpholino-9H-purin-8-yl)methyl)piperazin-2-one (**8o**). White solid, yield: 53%.  $^1\text{H}$  NMR (400 MHz,  $\text{CDCl}_3$ )  $\delta$  8.05–7.95 (m, 1H), 7.81–7.69 (m, 1H), 7.31–7.21 (m, 2H), 4.89 (s, 2H), 4.35 (s br, 6H), 3.95–3.82 (m, 9H), 3.57 (s, 2H), 3.35 (q,  $J = 7.5$  Hz, 2H), 1.74–1.58 (m, 1H), 1.44 (t,  $J = 7.5$  Hz, 3H), 1.04–1.00 (m, 2H), 0.91–0.77 (m, 2H).  $^{13}\text{C}$  NMR (101 MHz,  $\text{CDCl}_3$ )  $\delta$  172.0, 165.1, 156.93, 153.68, 153.41, 150.84, 145.15, 142.38, 134.49, 122.94, 122.77, 119.02, 117.30, 113.24, 66.98 (2C), 48.97, 46.63, 46.02 (2C), 42.48, 39.04, 29.27, 23.75, 12.38, 11.12, 8.23. ESI-MS  $[\text{M} + \text{H}]^+$  ( $m/z$ ): 544.3.

4-(cyclobutanecarbonyl)-1-((2-(2-ethyl-1H-benzo[d]imidazol-1-yl)-9-methyl-6-morpholino-9H-purin-8-yl)methyl)piperazin-2-one (**8p**). White solid, yield: 65%.  $^1\text{H}$  NMR (400 MHz,  $\text{CDCl}_3$ )  $\delta$  8.04–7.96 (m, 1H), 7.80–7.72 (m, 1H), 7.32–7.22 (m, 2H), 4.87 (s, 2H), 4.35 (s br, 4H), 4.11 (s, 1H), 3.95–3.78 (m, 9H), 3.61 (s, 1H), 3.54 (t,  $J = 6.5$  Hz, 2H), 3.35 (q,  $J = 7.5$  Hz, 2H), 3.29–3.19 (m, 1H), 2.41–1.95 (m, 6H), 1.44 (t,  $J = 7.5$  Hz, 3H).  $^{13}\text{C}$  NMR (101 MHz,  $\text{CDCl}_3$ )  $\delta$  173.24, 164.90, 156.90, 153.67, 153.40, 150.84, 145.58, 142.36, 134.48, 122.94, 122.78, 119.03, 117.28, 113.22, 66.97 (2C), 48.55, 46.64, 46.06 (2C), 42.47, 38.80, 37.11, 29.22, 24.89 (2C), 23.75, 17.91, 12.37. ESI-MS  $[\text{M} + \text{H}]^+$  ( $m/z$ ): 558.3. HRMS  $m/z$  calculated for  $\text{C}_{29}\text{H}_{36}\text{N}_9\text{O}_3^+$   $[\text{M} + \text{H}]^+$ : 574.2936, found 558.2948.

4-(cyclopentane carbonyl)-1-((2-(2-ethyl-1H-benzo[d]imidazol-1-yl)-9-methyl-6-morpholino-9H-purin-8-yl)methyl)piperazin-2-one (**8q**). White solid, yield: 49%.  $^1\text{H}$  NMR (400 MHz,  $\text{CDCl}_3$ )  $\delta$  7.99 (dd,  $J = 5.7, 3.2$  Hz, 1H), 7.81–7.71 (m, 1H), 7.35–7.20 (m, 2H), 4.88 (s, 2H), 4.47–4.16 (m, 6H), 3.90–3.83 (m, 9H), 3.63–3.49 (m, 2H), 3.35 (q,  $J = 7.5$  Hz, 2H), 2.96–2.70 (m, 1H), 1.89–1.69 (m, 6H), 1.65–1.53 (m, 2H), 1.43 (t,  $J = 7.5$  Hz, 3H).  $^{13}\text{C}$  NMR (101 MHz,  $\text{CDCl}_3$ )  $\delta$  174.70, 165.0, 156.96, 153.69, 153.41, 150.83, 145.60, 142.29, 134.46, 122.96, 122.80, 119.03, 117.30, 113.22, 66.98 (2C), 49.13, 46.52, 46.10 (2C), 42.48, 41.28, 38.94, 30.00 (2C), 29.23, 26.04 (2C), 23.69, 12.40. ESI-MS  $[\text{M} + \text{H}]^+$  ( $m/z$ ): 572.3.

1-((2-(2-ethyl-1H-benzo[d]imidazol-1-yl)-9-methyl-6-morpholino-9H-purin-8-yl)methyl)-4-(methylsulfonyl)piperazin-2-one (**8r**). White solid, yield: 57%.  $^1\text{H}$  NMR (400 MHz,  $\text{CDCl}_3$ )  $\delta$  8.08–7.95 (m, 1H), 7.84–7.69 (m, 1H), 7.28 (q,  $J = 5.8$  Hz, 2H), 4.88 (s, 2H), 4.35 (s br, 4H), 4.00 (s, 2H), 3.92–3.72 (m, 7H), 3.66 (d,  $J = 5.4$  Hz, 2H), 3.55 (t,  $J = 5.4$  Hz, 2H), 3.35 (q,  $J = 7.5$  Hz, 2H), 2.89 (s, 3H), 1.44 (t,  $J = 7.5$  Hz, 3H).  $^{13}\text{C}$  NMR (101 MHz,  $\text{CDCl}_3$ )  $\delta$  163.99, 156.92, 153.71, 153.41, 150.93, 145.45, 142.54, 134.55, 122.90, 122.73, 119.10, 117.27, 113.23, 66.98 (2C), 48.63, 46.78 (2C), 45.83, 42.66, 42.40, 36.41, 29.25, 23.81, 12.37. ESI-MS  $[\text{M} + \text{H}]^+$  ( $m/z$ ): 554.2.

1-((2-(2-ethyl-1H-benzo[d]imidazol-1-yl)-9-methyl-6-morpholino-9H-purin-8-yl)methyl)-4-(propylsulfonyl)piperazin-2-one (**8s**). White solid, yield: 51%.  $^1\text{H}$  NMR (400 MHz,  $\text{CDCl}_3$ )  $\delta$  8.00 (dd,  $J = 7.5, 2.1$  Hz, 1H), 7.82–7.70 (m, 1H), 7.32–7.21 (m, 2H), 4.88 (s, 2H), 4.34 (s br, 4H), 4.04 (s, 2H), 3.86 (d,  $J = 8.1$  Hz, 7H), 3.70–3.52 (m, 4H), 3.35 (q,  $J = 7.4$  Hz, 2H), 3.04–2.91 (m, 2H), 1.92–1.76 (m, 2H), 1.44 (t,  $J = 7.4$  Hz, 3H), 1.07 (t,  $J = 7.4$  Hz, 3H).  $^{13}\text{C}$  NMR (101 MHz,  $\text{CDCl}_3$ )  $\delta$  164.26, 156.91, 153.70, 153.43, 150.89, 145.50, 142.46, 134.52, 122.91, 122.75, 119.08, 117.28, 113.23, 66.99 (2C), 52.68, 48.59, 47.09 (2C), 45.89, 42.73, 42.47, 29.24, 23.78, 16.98, 13.00, 12.37. ESI-MS  $[\text{M} + \text{H}]^+$  ( $m/z$ ): 582.3.

4-(cyclopropylsulfonyl)-1-((2-(2-ethyl-1H-benzo[d]imidazol-1-yl)-9-methyl-6-morpholino-9H-purin-8-yl)methyl)piperazin-2-one (**8t**). White solid, yield: 62%.  $^1\text{H}$  NMR (400 MHz,  $\text{CDCl}_3$ )  $\delta$  8.08–7.96 (m, 1H),

7.81–7.71 (m, 1H), 7.35–7.22 (m, 2H), 4.88 (s, 2H), 4.35 (s, 4H), 4.06 (s, 2H), 3.94–3.78 (m, 7H), 3.72–3.55 (m, 4H), 3.35 (q,  $J = 7.5$  Hz, 2H), 2.37–2.25 (m, 1H), 1.44 (t,  $J = 7.5$  Hz, 3H), 1.25–1.19 (m, 2H), 1.10–0.99 (m, 2H).  $^{13}\text{C}$  NMR (101 MHz,  $\text{CDCl}_3$ )  $\delta$  164.25, 156.91, 153.71, 153.42, 150.91, 145.52, 142.46, 134.52, 122.91, 122.75, 119.09, 117.27, 113.24, 66.98 (2C), 49.08, 46.83 (2C), 45.88, 43.02, 42.36, 29.27, 26.58, 23.79, 12.38, 4.79 (2C). ESI-MS  $[\text{M}+\text{H}]^+$  ( $m/z$ ): 580.3.

### 3.2. Kinase assay

The inhibitory activity of **WNY1613** against 300 diverse human protein kinases including PI3K family was assessed by Reaction Biology Corp. Activity of individual kinases was evaluated by the Hot Spot assay platform, which contains specific kinase/substrate pairs and required cofactors [27]. The reaction mixture, which containing the compound and  $^{33}\text{P}$ -ATP, was incubated at 25°C for 2 h and spotted onto P81 ion exchange paper and the kinase activity was measured as  $^{33}\text{P}$  intensity of the spots. The extent of the kinase activity was indicated as a percentage of the kinase activity obtained without the compound. The inhibition rates were defined as the percentage of the kinase activity decreasing in the presence of the compound. The inhibition rate of **WNY1613** on all the tested kinases were listed in the [Supplementary material](#).

### 3.3. Thermal shift assay

Thermal shift assay was concluded to evaluate whether **WNY1613** binds with PI3K $\delta$  protein [20]. SU-DHL-6 and JEKO-1 cells were harvested, washed with PBS, and lysed by RIPA lysis buffer containing cocktail (1:1000). Next, centrifugation at 13000 rpm at 4 °C for 20 min and separated the soluble fraction (lysate) from the cell debris, which were then divided into two aliquots, with one aliquot being treated with **WNY1613** (10  $\mu\text{M}$ ) and the other aliquot with control. After 30 min of incubation at 25°C, the respective lysates were divided into individual 50  $\mu\text{L}$  aliquots and heated at different temperatures (35, 40, 45, 50, 55, 60, 70, 80, 90, 100 °C) for 6 min and then cooled at 25°C for 3 min. Then the heated lysates were centrifuged at 20000 rpm at 4 °C for 20 min and removed the denatured proteins, transferring 20  $\mu\text{L}$  of supernatants into new microtubes and analyzed by immunoblotting analysis to determine the degradation temperature of PI3K $\delta$  protein under **WNY1613** or control treatment.

### 3.4. Molecular modelling

The 3D structures of the PI3K $\delta$  and PI3K $\gamma$  were downloaded from the PDB (<http://www.rcsb.org/>, PDB ID: 2WXP, 3DBS). The protein was prepared with Discovery Studio 3.1 and the ligand **WNY1613** was prepared with ChemBio3D and optimized at molecular mechanical level. Then **WNY1613** was docked to the hinge and affinity pocket of PI3K $\delta$  and PI3K $\gamma$  using Autodock 4.2,[28] and the results were visualized by Discovery Studio 3.1.

### 3.5. Cell culture and reagents

All cell lines were purchased from the Cell Bank of the Chinese Academy of Sciences (Shanghai, China) and were cultured in Rosewell Park Memorial Institute (RPMI) 1640 media supplemented with 20% FBS and Penicillin-Streptomycin under humidified conditions with 5%  $\text{CO}_2$  at 37 °C.

### 3.6. Cell proliferation assay

Cells were seeded in 96-well plates at  $6 \sim 8 \times 10^3$  cells per well with a total volume of 100  $\mu\text{L}$  media and incubated for 24 h. Then different doses of compounds in 100  $\mu\text{L}$  media were added to the cells. After indicated times, cell viability was determined using the CellTiter 96®

non-radioactive cell proliferation MTT (Promega, Madison, WI, USA) assay [29] for the SAR study in [Section 2.2](#) or the CellTiter 96® Aqueous MTS (Promega, Madison, WI, USA) assay [30] for the anti-proliferative activity study in [Section 2.5](#).

### 3.7. Cell apoptosis analysis

The cell apoptosis assay was conducted on flow cytometry (FCM) [31], and before analysis, cells were treated with Idelalisib or **WNY1613** for 72 h. Next, the cells were harvested and stained by an Annexin V-fluorescein isothiocyanate (FITC)/PI apoptosis detection kit (Roche, Indianapolis, IN, USA) according to the manufacturer's protocol. A minimum of  $1 \times 10^4$  cells was analyzed using BD FACSCanto™ II (BD Biosciences, San Jose, CA USA), the data was analyzed by FlowJo software (V10.4, Ashland, OR, USA).

### 3.8. Immunoblotting analysis

Cells were treated by Idelalisib or **WNY1613** for indicated time and then were harvested and washed with PBS. The harvested cells were lysed in RIPA buffer (Beyotime, Beijing, China) contained phosphatase inhibitors (Roche, Basel, CH) and cocktail (1:1000) for 30 min and equalized before loading. The samples were separated by SDS-PAGE gel and transferred onto nitrocellulose (NC) filter membranes (Merck Millipore, MS, USA). Then the membranes were incubated with appropriate primary antibody overnight at 4°C, and then corresponding secondary antibody [32]. Chemiluminescence detection were used to detect specific protein bands. The antibodies used in this article are listed in the [Supplementary material](#).

### 3.9. Xenograft mouse model

All animal experiments have been approved by the Institutional Animal Care and Treatment Committee of Sichuan University in China (Permit Number: 20170135) and were carried out in accordance with the approved guidelines. NOD-SCID (6- to 9-week-old) mice [33] used in this study were purchased from Beijing HFK bioscience Co. LTD, Beijing, China and were performed in a specific-pathogen-free (SPF) condition facility. Mice injected subcutaneously with  $\sim 1 \times 10^7$  SU-DHL-6 or JEKO-1 cells were randomly divided into four groups: (i) Vehicle (Vehicle,  $n = 4$ ); (ii) Idelalisib (25 mg/kg,  $n = 4$ ); (iii) **WNY1613** (25 mg/kg,  $n = 4$ ); (iiii) **WNY1613** (50 mg/kg,  $n = 4$ ). Treatment group or the Vehicle consisting of 10% castor oil normal saline (NS) solution, 2.5% ethyl alcohol, 2.5% DMSO was administered at the indicated doses once a day for 18 or 21 days by oral gavage. Two diameters of tumors measured by electronic slide caliper every three days and tumor volumes were calculated using the following formula: tumor volume ( $\text{mm}^3$ ) =  $0.52 \times \text{length} \times \text{width}^2$ . The TGI values were calculated with the following formula:  $\text{TGI} = [1 - (\text{T}_n - \text{T}_0) / (\text{C}_n - \text{C}_0)] \times 100\%$ ,  $\text{T}_0$  and  $\text{T}_n$  represent average tumor volume before treatment and that of  $n$  days after treatment.  $\text{C}_0$  and  $\text{C}_n$  represent average tumor volume before treatment and that of  $n$  days after treatment in vehicle group.

### 3.10. Immunohistochemistry (IHC) analysis

Tumor tissues were fixed in 4% paraformaldehyde overnight and embedded in paraffin. Sections were subjected to immunohistochemical staining with antibody after cut into 5  $\mu\text{m}$  sections [32]. The antibodies used in this article are listed in the [Supplementary material](#).

### 3.11. Statistical analysis

The Student's  $t$ -test was used to examine statistically significant differences and all quantitative results are expressed as mean values  $\pm$  SD.  $P < 0.05$  indicates statistically significant.

## Declaration of Competing Interest

The authors declare that they have no known competing financial interests or personal relationships that could have appeared to influence the work reported in this paper.

## Acknowledgements

This work was supported by the Fundamental Research Funds for the Central Universities (No. 2682018CX37).

## Appendix A. Supplementary material

Supplementary data to this article can be found online at <https://doi.org/10.1016/j.bioorg.2020.104344>.

## References

- [1] L.C. Cantley, The phosphoinositide 3-kinase pathway, *Science* 296 (5573) (2002) 1655–1657.
- [2] R. Fritsch, J. Downward, SnapShot: class I PI3K isoform signaling, *Cell* 154 (4) (2013) 940.
- [3] D. Chantry, A. Vojtek, A. Kashishian, D.A. Holtzman, C. Wood, P.W. Gray, J. A. Cooper, M.F. Hoekstra, p110 $\delta$ , a novel phosphatidylinositol 3-kinase catalytic subunit that associates with p85 and is expressed predominantly in leukocytes, *J. Biol. Chem.* 272 (31) (1997) 19236–19241.
- [4] B. Vanhaesebroeck, M.J. Welham, K. Kotani, R. Stein, P.H. Warne, M.J. Zvelebil, K. Higashi, S. Volinia, J. Downward, M.D. Waterfield, p110 $\delta$ , a novel phosphoinositide 3-kinase in leukocytes, *Proc. Natl. Acad. Sci. USA* 94 (9) (1997) 4330–4335.
- [5] S.T. Jou, N. Carpino, Y. Takahashi, R. Piekorz, J.R. Chao, N. Carpino, D. Wang, J. N. Ihle, Essential, nonredundant role for the phosphoinositide 3-kinase p110 $\delta$  in signaling by the B-cell receptor complex, *Mol. Cell Biol.* 22 (24) (2002) 8580–8591.
- [6] K. Blajec, A. Borgstrom, A. Arcaro, Phosphatidylinositol 3-kinase isoforms as novel drug targets, *Curr. Drug Targets* 12 (7) (2011) 1056–1081.
- [7] D.A. Fruman, C. Rommel, PI3K $\delta$  inhibitors in cancer: rationale and serendipity merge in the clinic, *Can. Discov.* 1 (7) (2011) 562–572.
- [8] D.L. Kienle, S. Stilgenbauer, Approved and emerging PI3K inhibitors for the treatment of chronic lymphocytic leukemia and non-Hodgkin lymphoma, *Expert Opin. Pharmacol.* 21 (8) (2020) 1–13.
- [9] Y. Feng, X. Cu, M. Xin, PI3K $\delta$  inhibitors for the treatment of cancer: a patent review (2015–present), *Expert Opin. Ther. Pat.* 29 (12) (2019) 925–941.
- [10] C.Y. Cheah, N.H. Fowler, Idelalisib in the management of lymphoma, *Blood* 128 (3) (2016) 331–336.
- [11] I.W. Flinn, S. O'Brien, B. Kahl, M. Patel, Y. Oki, F.F. Foss, P. Porcu, J. Jones, J. A. Burger, N. Jain, Duvelisib, a novel oral dual inhibitor of PI3K- $\delta$ ,  $\gamma$ , is clinically active in advanced hematologic malignancies, *Blood* 131 (8) (2018) 877–887.
- [12] M. Dreyling, A. Santoro, L. Mollica, S. Leppä, G.A. Follows, G. Lenz, W.S. Kim, A. Nagler, P. Panayiotidis, J. Demeter, Phosphatidylinositol 3-Kinase Inhibition by Copanlisib in Relapsed or Refractory Indolent Lymphoma, *J. Clin. Oncol.* 35 (35) (2017) 3898–3905.
- [13] C.L. Lucas, A. Chandra, S. Nejentsev, A.M. Condliffe, K. Okkenhaug, PI3K $\delta$  and primary immunodeficiencies, *Nat. Rev. Immunol.* 16 (11) (2016) 702–714.
- [14] N.Y. Wang, W.Q. Zuo, R. Hu, W.L. Wang, Y.X. Zhu, Y. Xu, L.T. Yu, Z.H. Liu, Design, synthesis and structure-activity relationship study of piperazinone-containing thieno[3,2-d]pyrimidine derivatives as new PI3K $\delta$  inhibitors, *Bioorg. Med. Chem. Lett.* 30 (20) (2020), 127479.
- [15] J.M. Murray, Z.K. Sweeney, B.K. Chan, M. Balazs, E. Bradley, G. Castanedo, C. Chabot, D. Chantry, M. Flagella, D.M. Goldstein, R. Kondru, J. Lesnick, J. Li, M. C. Lucas, J. Nonomiya, J. Pang, S. Price, L. Salphati, B. Safina, P.P.A. Savy, E. M. Seward, M. Ulsch, D.P. Sutherland, Potent and highly selective benzimidazole inhibitors of PI3-kinase delta, *J. Med. Chem.* 55 (17) (2012) 7686–7695.
- [16] B.S. Safina, Z.K. Sweeney, J. Li, Br.K. Chan, A. Bisconte, D. Carrera, G. Castanedo, M. Flagella, R. Heald, C. Lewis, J.M. Murray, J. Nonomiya, J. Pang, S. Price, K. Reif, L. Salphati, E.M. Seward, B. Wei, D.P. Sutherland, Identification of GNE-293, a potent and selective PI3K $\delta$  inhibitor: navigating in vitro genotoxicity while improving potency and selectivity, *Bioorg. Med. Chem. Lett.* 23 (17) (2013) 4953–4959.
- [17] N.Y. Wang, Y. Xu, W.Q. Zuo, K.J. Xiao, L. Liu, X.X. Zeng, X.Y. You, L.D. Zhang, C. Gao, Z.H. Liu, T.H. Ye, Y. Xia, Y. Xiong, X.J. Song, Q. Lei, C.T. Peng, H. Tang, S. Y. Yang, Y.Q. Wei, L.T. Yu, Discovery of imidazo[2,1-b]thiazole HCV NS4B inhibitors exhibiting synergistic effect with other direct-acting antiviral agents, *J. Med. Chem.* 58 (6) (2015) 2764–2778.
- [18] F.I. Raynaud, S.A. Eccles, S. Patel, S. Alix, G. Box, I. Chuckowree, A. Folkes, S. Gowan, A.D.H. Brandon, F.D. Stefano, A. Hayes, A.T. Henley, L. Lensun, G. Pergl-Wilson, A. Robson, N. Saghir, A. Zhyvoloup, E. McDonald, P. Shelldrake, S. Shuttleworth, M. Valenti, N.C. Wan, P.A. Clarke, P. Workman, Biological properties of potent inhibitors of class I phosphatidylinositol 3-kinases: from PI-103 through PI-540, PI-620 to the oral agent GDC-0941, *Mol. Cancer Ther.* 8 (7) (2009) 1725–1738.
- [19] B.J. Lannutti, S.A. Meadows, S.E.M. Herman, A. Kashishian, B. Steiner, A. J. Johnson, J.C. Byrd, J.W. Tyner, M.M. Loriaux, M. Deininger, B.J. Druker, K. D. Puri, R.G. Ulrich, N.A. Giese, CAL-101, a p110 $\delta$  selective phosphatidylinositol-3-kinase inhibitor for the treatment of B-cell malignancies, inhibits PI3K signaling and cellular viability, *Blood* 117 (2) (2011) 591–594.
- [20] D.M. Molina, R. Jafari, M. Ignatshchenko, T. Seki, E.A. Larsson, C. Dan, L. Sreekumar, Y. Cao, P. Nordlund, Monitoring drug target engagement in cells and tissues using the cellular thermal shift assay, *Science* 341 (6141) (2013) 84–87.
- [21] A.J. Folkes, K. Ahmadi, W.K. Alderton, S. Alix, S.J. Baker, G. Box, I.S. Chuckowree, P.A. Clarke, P. Depledge, S.A. Eccles, L.S. Friedman, A. Hayes, T.C. Hancox, A. Kugendradas, L. Lensun, P. Moore, A.G. Olivero, J. Pang, S. Patel, G.H. Pergl-Wilson, F.I. Raynaud, A. Robson, N. Saghir, L. Salphati, S. Sohal, M.H. Ulsch, M. Valenti, H.J.A. Wallweber, N.C. Wan, C. Wiesmann, P. Workman, A. Zhyvoloup, M.J. Zvelebil, S.J. Shuttleworth, The identification of 2-(1H-indazol-4-yl)-6-(4-methanesulfonyl-piperazin-1-ylmethyl)-4-morpholin-4-yl-thieno[3,2-d]pyrimidine (GDC-0941) as a potent, selective, orally bioavailable inhibitor of class I PI3 kinase for the treatment of cancer, *J. Med. Chem.* 51 (18) (2008) 5522–5532.
- [22] A. Berndt, S. Miller, O. Williams, D.D. Le, B.T. Housema, J.I. Pacold, F. Gorrec, W.-C. Hon, P. Ren, Y. Liu, C. Rommel, P. Gaillard, T. Rückle, M.K. Schwarz, K. M. Shokat, J.P. Shaw, R.L. Williams, The p110 $\delta$  structure: mechanisms for selectivity and potency of new PI(3)K inhibitors, *Nat. Chem. Biol.* 6 (2) (2010) 117–124.
- [23] S. Fulda, Modulation of mitochondrial apoptosis by PI3K inhibitors, *Mitochondrion* 13 (3) (2013) 195–198.
- [24] M. Will, A.C.R. Qin, W. Toy, Z. Yao, V. Rodrik-Outmezguine, C. Schneider, X. Huang, P. Monian, X. Jiang, E. de Stanchina, J. Baselga, N. Liu, S. Chandralapaty, N. Rosen, Rapid induction of apoptosis by PI3K inhibitors is dependent upon their transient inhibition of RAS-ERK signaling, *Cancer Discov.* 4 (3) (2014) 334–347.
- [25] H. Ebi, C. Costa, A.C. Faber, M. Nishitani, H. Kotani, D. Juric, P.D. Pelle, Y. Song, S. Yano, M. Mino-Kenudson, C.H. Benes, J.A. Engelman, PI3K regulates MEK/ERK signaling in breast cancer via the Rac-GEF, P-Rex1, *Proc. Natl. Acad. Sci. USA* 110 (52) (2013) 21124–21129.
- [26] G. Castanedo, B. Chan, D. M. Goldstein, R. K. Kondru, M. C. Lucas, W. S. Palmer, S. Price, B. Safina, P. P. A. Savy, E. M. Seward, D. P. Sutherland, Z. K. Sweeney, Preparation of bicyclic pyrimidines as selective inhibitors of the p110 delta isoform of PI3K for treating inflammation, immune diseases and cancers, *WO 2010138589*, May 26 (2010).
- [27] T. Anastassiadis, S.W. Deacon, K. Devarajan, H. Ma, J.R. Peterson, Comprehensive assay of kinase catalytic activity reveals features of kinase inhibitor selectivity, *Nat. Biotechnol.* 29 (11) (2011) 1039–1045.
- [28] G.M. Morris, R. Huey, W. Lindstrom, M.F. Sanner, R.K. Bewle, D.S. Goodsell, A. J. Olson, AutoDock4 and AutoDockTools4: automated docking with selective receptor flexibility, *J. Comput. Chem.* 30 (16) (2009) 2785–2791.
- [29] T. Hideshima, D. Chauhan, T. Hayashi, K. Podar, M. Akiyama, C. Mitsiades, N. Mitsiades, B. Gong, L. Bonham, P. de Vries, N. Munshi, P.G. Richardson, J. W. Singer, K. C. Anderson, Antitumor activity of lysophosphatidic acid acyltransferase-beta inhibitors, a novel class of agents, in multiple myeloma, *Can. Res.* 63 (23) (2003) 8428–8436.
- [30] L.A.M. Grinera, R. Guhaa, P. Shinna, R.M. Young, J.M. Keller, D. Liu, I.S. Goldlust, A. Yasgar, C. McKnight, M.B. Boxer, D.Y. Dubeau, J.-K. Jiang, S. Michael, T. Mierzwa, W. Huang, M.J. Walsh, B.T. Mott, P. Patel, W. Leister, D.J. Maloney, C. A. Leclair, G. Rai, A. Jadhav, B.D. Peyser, C.P. Austin, S.E. Martin, A. Simeonov, M. Ferrer, L.M. Staudt, C.J. Thomas, High-throughput combinatorial screening identifies drugs that cooperate with ibrutinib to kill activated B-cell-like diffuse large B-cell lymphoma cells, *Proc. Natl. Acad. Sci. USA* 111 (6) (2014) 2349–2354.
- [31] L.S. Chen, S. Redkar, D. Bearss, W.G. Wierda, V. Gandhi, Pim kinase inhibitor, SGI-1776, induces apoptosis in chronic lymphocytic leukemia cells, *Blood* 114 (19) (2009) 4150–4157.
- [32] Y. Xu, Q. Wang, K. Xiao, Z. Liu, L. Zhao, X. Song, X. Hu, Z. Feng, T. Gao, W. Zuo, J. Zeng, N. Wang, L. Yu, novel dual BET and PLK1 inhibitor WNY0824 exerts potent antitumor effects in CRPC by inhibiting transcription factor function and inducing mitotic abnormality, *Mol. Cancer Ther.* 19 (6) (2020) 1221–1231.
- [33] L.D. Shultz, P.A. Schweitzer, S.W. Christianson, B. Gott, I.B. Schweitzer, B. Tennent, S. McKenna, L. Mobraaten, T.V. Rajan, D.L. Greiner, Multiple defects in innate and adaptive immunologic function in NOD/LtSz-scid mice, *J. Immunol.* 154 (1) (1995) 180–191.